



Calhoun: The NPS Institutional Archive
DSpace Repository

Theses and Dissertations

1. Thesis and Dissertation Collection, all items

1993-06

Stability curves for a thermoacoustic prime mover

Kuo, Fan-Ming

Monterey, California. Naval Postgraduate School

<http://hdl.handle.net/10945/39801>

Copyright is reserved by the copyright owner.

Downloaded from NPS Archive: Calhoun



Calhoun is the Naval Postgraduate School's public access digital repository for research materials and institutional publications created by the NPS community. Calhoun is named for Professor of Mathematics Guy K. Calhoun, NPS's first appointed -- and published -- scholarly author.

Dudley Knox Library / Naval Postgraduate School
411 Dyer Road / 1 University Circle
Monterey, California USA 93943

<http://www.nps.edu/library>

NAVAL POSTGRADUATE SCHOOL
Monterey, California

2

AD-A272 607



S DTIC
ELECTE
NOV 16 1993
A

THESIS

**STABILITY CURVES FOR A THERMOACOUSTIC PRIME
MOVER**

by

Kuo, Fan-Ming

June 1993

Thesis Advisor:
Co-Advisor:

Anthony A. Atchley
Robert M. Keolian

Approved for public release; distribution is unlimited.

93-27767



REPORT DOCUMENTATION PAGE

1a. REPORT SECURITY CLASSIFICATION UNCLASSIFIED		1b. RESTRICTIVE MARKINGS	
2a. SECURITY CLASSIFICATION AUTHORITY		3. DISTRIBUTION/AVAILABILITY OF REPORT Approved for public release; distribution is unlimited	
2b. DECLASSIFICATION/DOWNGRADING SCHEDULE			
4. PERFORMING ORGANIZATION REPORT NUMBER(S)		5. MONITORING ORGANIZATION REPORT NUMBER(S)	
6a. NAME OF PERFORMING ORGANIZATION Physics Dept. Naval Postgraduate School	6b. OFFICE SYMBOL (if applicable) PH	7a. NAME OF MONITORING ORGANIZATION Naval Postgraduate School	
6c. ADDRESS (City, State, and ZIP Code) Monterey, CA 93943-5000		7b. ADDRESS (City, State, and ZIP Code) Monterey, CA 93943-5000	
8a. NAME OF FUNDING/SPONSORING ORGANIZATION	8b. OFFICE SYMBOL (if applicable)	9. PROCUREMENT INSTRUMENT IDENTIFICATION NUMBER	
8c. ADDRESS (City, State, and ZIP Code)		10. SOURCE OF FUNDING NUMBERS	
		PROGRAM ELEMENT NO.	PROJECT NO.
		TASK NO.	WORK UNIT ACCESSION NO.
11. TITLE (Include Security Classification) STABILITY CURVES FOR A THERMOACOUSTIC PRIME MOVER			
12. PERSONAL AUTHOR(S) Kuo, Fan-Ming			
13a. TYPE OF REPORT Master's Thesis	13b. TIME COVERED FROM TO	14. DATE OF REPORT (Year, Month, Day) June 1993	15. PAGE COUNT 45
16. SUPPLEMENTARY NOTATION The views expressed in this thesis are those of the author and do not reflect the official policy or position of the Department of Defense or the United States Government.			
17. COSATI CODES		18. SUBJECT TERMS (Continue on reverse if necessary and identify by block number)	
FIELD	GROUP	Acoustics, Thermoacoustics, Prime Mover, Stability Curves, Quasiperiodic	
19. ABSTRACT (Continue on reverse if necessary and identify by block number) The purpose of this thesis is to investigate the stability curves for and steady state waveforms in a helium filled prime mover for both the fundamental and second modes. The predicted and measured stability limits are in reasonable agreement for both modes at most mean pressures. There is, however, evidence that the stability of one mode is affected by the presence of the other. It is also observed that one mode can suppress the other. Measurements were also made on a prime mover modified such the fundamental mode was selectively inhibited. Results indicate that the reduced fundamental amplitude allows the stability curve for the second mode to extend into the regions where the fundamental mode previously dominated. This produces a region where both modes are simultaneously excited. Analysis of the waveforms show that the resulting oscillations are quasiperiodic.			
20. DISTRIBUTION/AVAILABILITY OF ABSTRACT <input checked="" type="checkbox"/> UNCLASSIFIED/UNLIMITED <input type="checkbox"/> SAME AS RPT. <input type="checkbox"/> DTIC USERS		21. ABSTRACT SECURITY CLASSIFICATION UNCLASSIFIED	
22a. NAME OF RESPONSIBLE INDIVIDUAL Anthony A. Atchley		22b. TELEPHONE (Include Area Code) (408) 656-2848	22c. OFFICE SYMBOL PH/Ay

Approved for public release; distribution is unlimited

STABILITY CURVES FOR A THERMOACOUSTIC PRIME MOVER

by
Kuo, Fan-Ming
Lt, Republic of China Navy
B.S., Chinese Naval Academy, 1989

Submitted in partial fulfillment of the
requirements for the degree of

MASTER OF SCIENCE IN ENGINEERING ACOUSTICS

from the

NAVAL POSTGRADUATE SCHOOL

June 1993

Author:

Kuo, Fan-Ming

Approved By:

Anthony A. Atchley, Thesis Advisor

Robert M. Keolian, Thesis Co-advisor

Anthony A. Atchley
Chairman, Engineering Acoustics Academic Committee

ABSTRACT

The purpose of this thesis is to investigate the stability curves for and steady state waveforms in a helium filled prime mover for both the fundamental and second modes. The predicted and measured stability limits are in reasonable agreement for both modes at most mean pressures. There is, however, evidence that the stability of one mode is affected by the presence of the other. It is also observed that one mode can suppress the other. Measurements were also made on a prime mover modified such that the fundamental mode was selectively inhibited. Results indicate that the reduced fundamental amplitude allows the stability curve for the second mode to extend into the regions where the fundamental mode previously dominated. This produces a region where both modes are simultaneously excited. Analysis of the waveforms show that the resulting oscillations are quasiperiodic.

Accession For	
NTIS CRA&I	<input checked="checked" type="checkbox"/>
DTIC TAB	<input type="checkbox"/>
Unannounced	<input type="checkbox"/>
Justification	
By	
Distribution /	
Availability Codes	
Dist	Avail and/or Special
A-1	

TABLE OF CONTENTS

I.	INTRODUCTION	1
II.	THEORY	3
A.	PREDICTION OF ONSET PARAMETERS	3
B.	QUASIPERIODIC AND CHAOSTIC STATES	7
III.	EXPERIMENTAL APPARATUS AND PROCEDURE	8
A.	EXPERIMENTAL APPARATUS	8
1.	The Prime Mover	8
a.	<i>The Ambient Duct, Ambient Heat Exchanger</i>	8
b.	<i>The Prime Mover Stack</i>	10
c.	<i>The Hot Duct and Hot Heat Exchanger</i>	10
2.	The Pressure Control System	10
3.	The Temperature Control System	11
4.	Data Acquisition System	12
B.	EXPERIMENTAL PROCEDURE AND DATA ACQUISITION	12
IV.	OBSERVATIONS, RESULTS AND DISCUSSIONS	14
A.	THE STABILITY CURVES	14
B.	ANALYSIS OF WAVEFORMS	20
V.	SUMMARY AND RECOMMENDATIONS	36
A.	SUMMARY	36
B.	RECOMMENDATIONS	37
	LIST OF REFERENCES	38
	INITIAL DISTRIBUTION LIST	39

I. INTRODUCTION

The transition to onset of self-oscillation in thermoacoustic prime movers can be considered in terms of the transition from a stable state to an unstable state. The stable state, below onset, is one for which the prime mover as a whole has a net positive damping. Any oscillations excited in a prime mover below onset decay in time. The behavior of prime movers below onset has been the topic of previous investigations. [Refs. 1-3] The unstable state, above onset, is one for which the damping is negative. Oscillations at the resonance frequency initially exhibit exponential growth in amplitude. Eventually steady state is obtained and the growth rate is zero. The steady state acoustic pressure amplitude is typically on the order of 10% or more of ambient pressure.

An extensive series of investigations on the behavior of a simple prime mover (although they didn't call it that) was conducted by Yazaki, et al. [Refs. 4-6] Their prime mover consisted of a symmetric stainless steel U-shaped tube (inner radius 1.2 - 4.7 mm, length 1.5 m and greater) with two small pressure transducers affixed at both closed ends. The cold section was immersed into the cold reservoir whose temperature was adjusted by a continuous flow of cold helium gas. The warm part was maintained at room temperature (293 K). They investigated both the limits of stability of their system as well as the highly nonlinear nature of the oscillations above onset. They discovered a wealth of complex behavior, including phase locking, mode competition, quasiperiodicity and chaos.

We have undertaken a similar investigation on a practical prime mover. In particular, we have concentrated on the excitation of the second longitudinal mode of the prime mover

and the simultaneous excitation of both the fundamental and second modes. The region of two mode excitation in practical prime mover has received little attention previously.

In Chapter II, the theory used to calculate the onset conditions is discussed in Section A. Section B contains a brief description of techniques for analyzing periodic and quasiperiodic waveforms. Experimental apparatus and procedure are discussed in Chap. III, followed by observations, results and discussions in Chap. IV. The last chapter will present a summary and recommendations.

II. THEORY

There are two aspects of this thesis. The first is investigating the stability curve for the fundamental and second modes of a prime mover. The important parameters for this study are the temperature difference required for onset ΔT_{onset} and the mean gas pressure in the prime mover P_m . Prediction of the stability curves is discussed in Sect. A. The second aspect is the investigation of the nature of the acoustic oscillations in the unstable regions of the parameter space. Techniques for analyzing these oscillations are discussed in Sect. B.

A. PREDICTION OF ONSET PARAMETERS

As depicted in Figure 1, the basic prime mover construction can be decomposed into five major sections: the ambient duct, the ambient heat exchanger, the prime mover stack, the hot heat exchanger, and the hot duct. We can evaluate the performance of prime movers and predict onset parameters in term of quality factor Q as discussed by Atchely and Lin [Refs. 1, 2]. The reader should refer to Ref. 1 and 2 for a full explanation. Only the important aspects will be deliberated here.

The quality factor Q of a resonator is defined as 2π times the ratio of the energy stored in the resonator to the energy dissipated per cycle. Thus, $1/Q$ can be expressed as

$$\frac{1}{Q} = \frac{\bar{E}}{\omega E_{ST}} \quad (1)$$

\bar{E} is the total dissipated acoustic power. E_{ST} denotes the stored energy. Both \bar{E} and E_{ST} are second order in the acoustic amplitude. ω is the angular frequency. We use the reciprocal

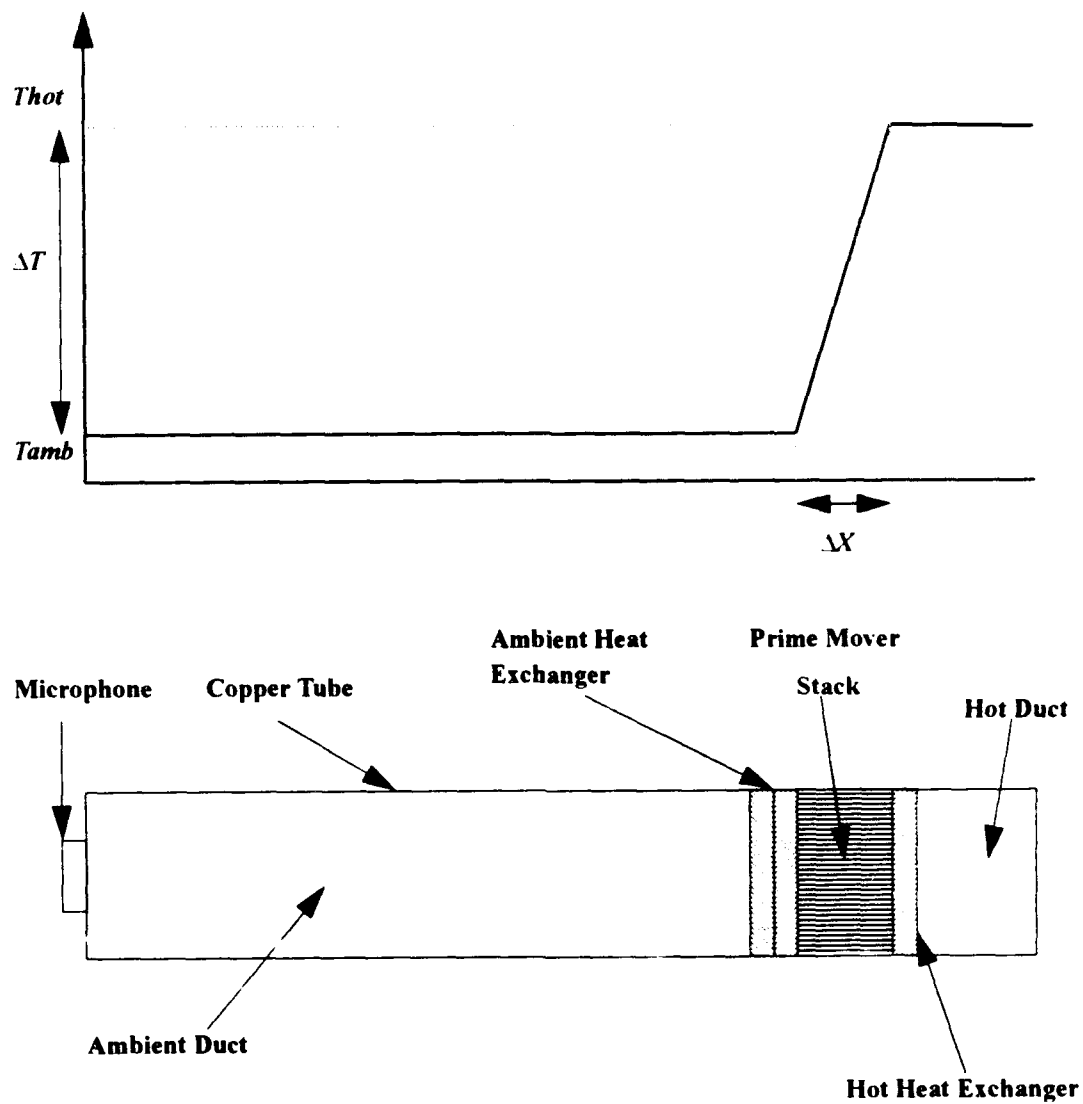


Figure 1 - Diagram of the basic prime mover configuration and mean temperature distribution.

of quality factor, since $1/Q$ is proportional to the acoustic power output of the prime mover and it will converge to zero at onset rather than diverge to infinity as does Q .

The analysis used in Ref. 1 calculates $1/Q$ based on thermoacoustic theory. $1/Q$ is a function of the prime mover geometry, the thermophysical properties of the gas, P_m and ΔT . Below onset $1/Q$ is positive. At onset $1/Q$ is zero. Above onset $1/Q$ is negative. For a given prime mover geometry and gas type, the temperature difference ΔT required for onset ΔT_{onset} is a function of ambient pressure P_m . A plot of ΔT_{onset} vs. P_m defines the so called stability curve for a prime mover. An example is shown in Fig. 2. In order for self-sustained oscillations to exist, both the control parameters P_m and ΔT_{onset} must lie within the unstable regions. This means that, for example, for a relative low mean gas pressure P_m , the temperature difference ΔT must be relatively high to reach onset. There are two reversible processes (isothermal and adiabatic processes) corresponding to the stability limits of prime mover. At the left branch of the stability curve, at extremely low gas pressure, the thermal boundary layer is big and the oscillations tend toward being isothermal. At high pressure, the thermal boundary layer is small and the oscillations tend toward being adiabatic. No heat flux is created in the isothermal or adiabatic reversible processes.

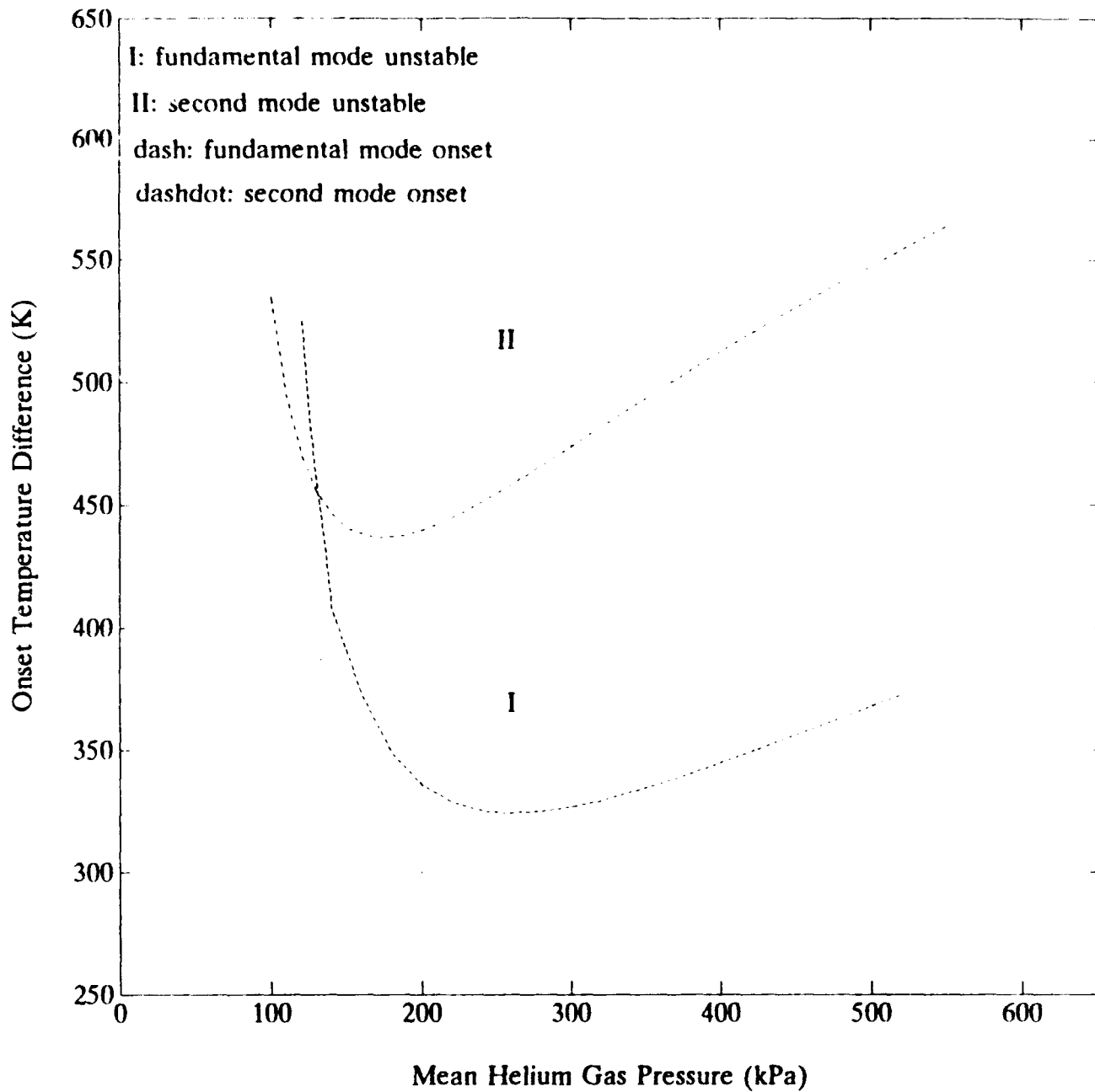


Fig. 2 - Theoretical stability curves for the fundamental and second modes of our prime mover filled with helium gas.

B. QUASIPERIODIC AND CHAOTIC STATES

In this thesis we will investigate the steady-state oscillations of the prime mover at different points in the $(P_m, \Delta T)$ parameter space. Because the high amplitude behavior can be highly nonlinear, we will use some methods developed for studying nonlinear dynamical systems. In particular, we will determine the phase portraits of the acoustic oscillations. Analysis of phase portraits allows one to distinguish among periodic, quasiperiodic and chaotic oscillations.

The phase portraits are constructed from digitized samples $x(t_i)$ of the continuous acoustic pressure waveform $x(t)$. Here the subscript i indicates that x is sampled at discrete times. There are several possible combinations of independent variables that can be used to construct phase portraits. [Ref. 7] We choose two. One is to plot $\dot{x}(t_i)$ vs. $x(t_i)$, where $\dot{x}(t_i)$ is the time derivative of $x(t_i)$. $\dot{x}(t_i)$ is computed according to $(x(t_i) - x(t_{i-1})) / (t_i - t_{i-1})$. The other phase portrait is constructed as $x(t_{i+1})$ vs. $x(t_i)$. In either case periodic oscillations are characterized by forming closed loops in phase space. As time goes on, the phase space trajectory traces over the same loop cycle after cycle. Quasiperiodic oscillations, on other hand, never repeat the same phase space trajectory.

III. EXPERIMENTAL APPARATUS AND PROCEDURE

We will measure ΔT_{onset} of the fundamental and second modes of the prime mover as a function of P_m . The acoustic stability curves can be determined from these measurements. Selected output signal waveforms are also analyzed.

The experimental apparatus consists of the following four parts: the prime mover in which the acoustic oscillations are thermally induced, the gas pressure control system which regulates helium gas pressure in the resonator, the temperature control system for producing and maintaining the temperature gradient across the prime mover stack, and the data acquisition system that displays, digitizes and records the output signals. These four parts are discussed in Section A 1, 2, 3, 4 respectively and schematically shown in Fig. 3. The experimental procedure and data acquisition are described in Section B.

A. EXPERIMENTAL APPARATUS

1. The Prime Mover

As depicted in Figure 1, the prime mover construction can be mainly decomposed into five major sections: the ambient duct, the ambient heat exchanger, the prime mover stack, the hot heat exchanger, and the hot duct. These sections are briefly described below. The reader is referred to Refs. 1, 2 and 3 for a complete description.

a. The Ambient Duct, Ambient Heat Exchanger

The ambient duct is an 88.11-cm-long, 3.82-cm-i.d. (inner diameter) copper tube. One end is flanged. A brass end cap is bolted to the flange and holds a piezoresistive,

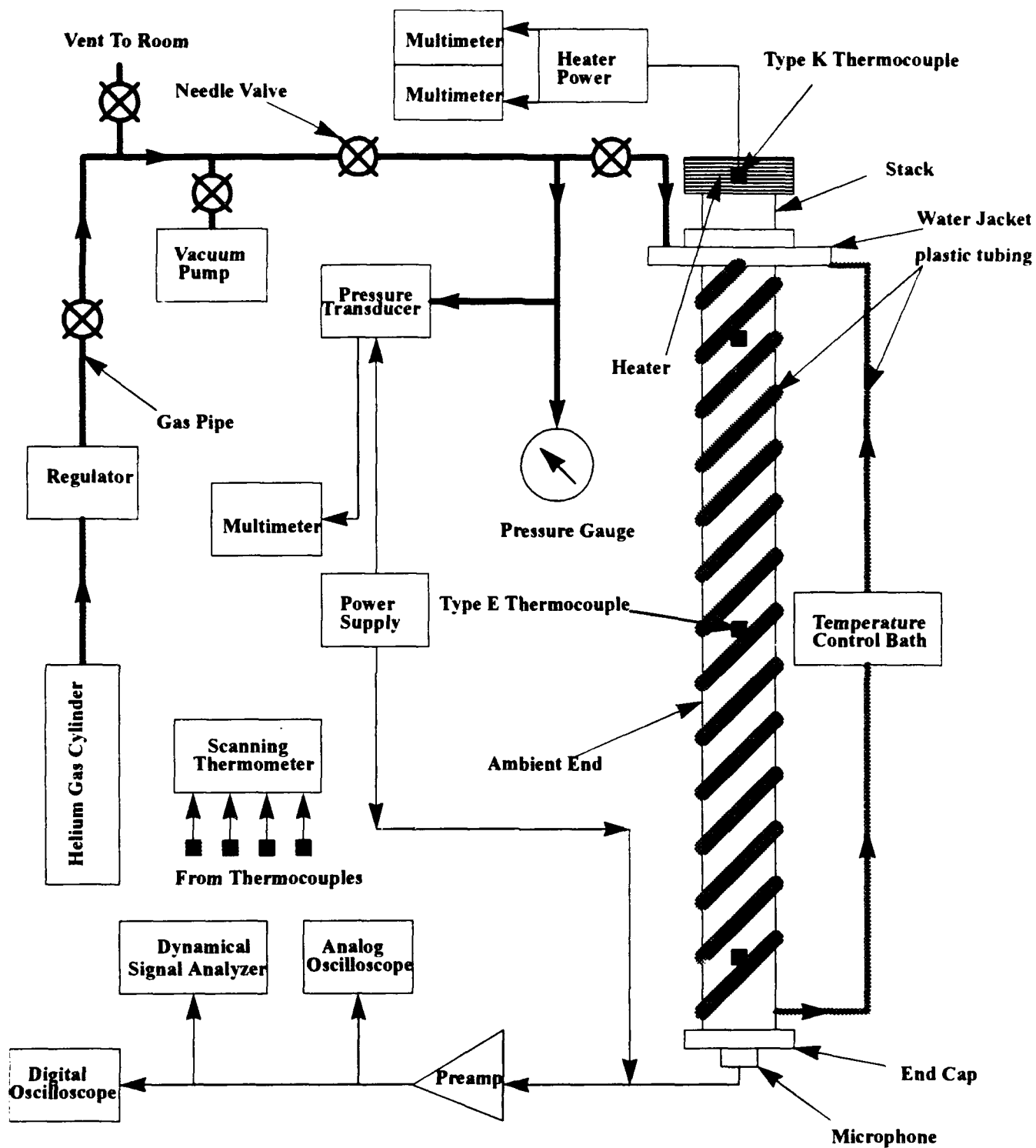


Figure 3 - Schematic diagram of the instrumentation used in the experiment.

high intensity microphone. The ambient heat exchanger is mounted in the ambient heat exchanger container and is comprised of two stacks of parallel plates. Each stack is comprised of twenty five, 1.02-cm-long, 0.045-cm-thick copper plates. The ambient heat exchanger container is soldered to one end of the ambient duct. A water jacket surrounds the ambient heat exchanger container.

b. The Prime Mover Stack

The prime mover stack is a cylindrical stainless steel shell filled with thirty five, 3.50-cm-long, 0.028-cm-thick, stainless steel plates spaced by about 0.077 cm. One end of the stack is soldered to the ambient heat exchanger container, such that the stack and ambient heat exchanger are in contact.

c. The Hot Duct and Hot Heat Exchanger

The hot duct of the prime mover is constructed from a 5.50-cm-long nickel tube with the same inner diameter as the ambient duct's. The hot heat exchanger is similar to the ambient heat exchanger except the plates are nickel and are 0.762 cm long. The hot heat exchanger is welded to both the hot duct and the stack. The other end of the hot duct is rigidly capped. The cap has a hole drilled at the center for accommodating a thermocouple probe. A type K thermocouple is inserted through the hole in hot duct, making contact with the hot heat exchanger. It is used for sensing the temperature of hot heat exchanger.

2. The Pressure Control System

The mean gas pressure in the prime mover is one of our control parameters. It ranges from 100 kPa to 540 kPa in our experiment. Because the performance of this prime

mover is strictly dependent upon the purity of the helium gas, before we start our experiment, we evacuate and pressurize the prime mover several times to ensure that the helium gas in the chamber is not contaminated by ambient air. A precise value of gas pressure is obtained by the adjustment of the gas flow rate through a regulator and several needle valves. The pressure is monitored with an Omega PX304-300AV pressure transducer. The dc voltage reading of the pressure transducer is displayed by a HP-3478A multimeter.

3. The Temperature Control System

The heat source for the prime mover is an Omega Engineering HBA Model 202040 heater powered by a 115 volt, 60 Hz, GR Type 100-Q adjustable transformer. The hot duct and hot heat exchanger assembly is firmly wrapped by heater coils and surrounded with an insulating jacket to reduce the heat loss to the room. The ambient heat exchanger is surrounded by a water jacket. Water from a Neslab Model RET-110 constant temperature bath is circulated through the jacket and through plastic tubing which is wrapped around the ambient duct. The bath provides a continuous flow of room temperature water to maintain a uniform temperature (approximately 20 °C).

A type K thermocouple is in contact with the hot heat exchanger to sense the temperature of the hot assembly. Three type E thermocouples are glued to the top, middle, and bottom, respectively, of the ambient section of the prime mover to sense the temperature distribution along the ambient assembly. The outputs of these four thermocouples are read with a Keithley 740 System scanning thermometer.

4. Data Acquisition System

When the prime mover reaches onset, the acoustic signal is detected by an ENDEVCO Model 8510B-5 piezoresistive pressure transducer located in the ambient end cap. DC pressure differences are equalized through a 0.0102-cm-i.d., high impedance capillary tube. The linear pressure response range of the transducer is ± 34.48 kPa. The output signal from the transducer is amplified by an AM502 differential amplifier and then sent to a Kikusui COS6100A oscilloscope, HP 3561A dynamical signal analyzer, and Nicolet Pro30 digital oscilloscope for signal displaying and data recording purposes.

B. EXPERIMENTAL PROCEDURE AND DATA ACQUISITION

The prime mover chamber was pressurized with the desired gas pressure which ranged from 100 kPa to 540 kPa at intervals of 20 kPa. The uncertainty of this control parameter is approximately $\pm 1\%$.

The ambient duct of the prime mover was maintained at near 293 K by circulating preset temperature water through the water jacket of the ambient heat exchanger and water pipe. Temperatures at the hot end could be varied continuously from 293 K to 560 K. Furthermore, for obtaining a more homogeneous temperature distribution along the ambient end, the RET-110 temperature control bath's preset temperature was decreased as the temperature of the heater was increased to maintain the room-temperature requirement. When the prime mover reached onset, the values of two control parameters P_m and ΔT_{onset} were recorded for further data analysis. This procedure was repeated until the control parameters reached their maximum limits.

In order to analyze the steady state oscillations, selected waveforms were recorded via Nicolet Pro30 digital oscilloscope. The samples contained 20000 points recorded at 50 μ s per point.

IV. OBSERVATIONS, RESULTS AND DISCUSSIONS

This chapter is divided into two sections. In Sec. A, we will present the stability curves. In Sec. B, we will analyze the representative waveforms.

A. THE STABILITY CURVES

The stability curves for the fundamental and second modes of the prime mover are shown in Fig. 4. The \circ 's indicate the measured onset conditions for the fundamental mode. The $*$'s indicate the measured onset conditions for the second mode. The $+$'s indicate the onset conditions for the fundamental mode, after the second mode is above onset. These last data points were obtained by fixing ΔT and increasing P_m . We estimate that the maximum error is ± 5 K for ΔT_{onset} and ± 1 to 2% for P_m . The solid lines are interpolations of the data. The dashed and dash-dot lines are the theoretical stability curve for the fundamental and second modes, respectively, based on the analysis from Ref. 1. It is seen that the predicted and measured stability limits are in reasonable agreement for the fundamental mode at most mean pressures. The predicted trend for the second mode is consistent with the measurements, yet the predicted values of ΔT_{onset} are higher than those measured. These results are generally consistent with those reported in Ref. 1.

There are, however, two more interesting aspects of Fig. 4. The first is that the slope of the stability curve for the fundamental is positive when the second mode is excited. (These points are represented by the $+$'s.) The predicted slope of the stability curve at low pressures is negative. It is not completely surprising that the slope is different than that predicted because the theoretical curves do not take into account the presence of other

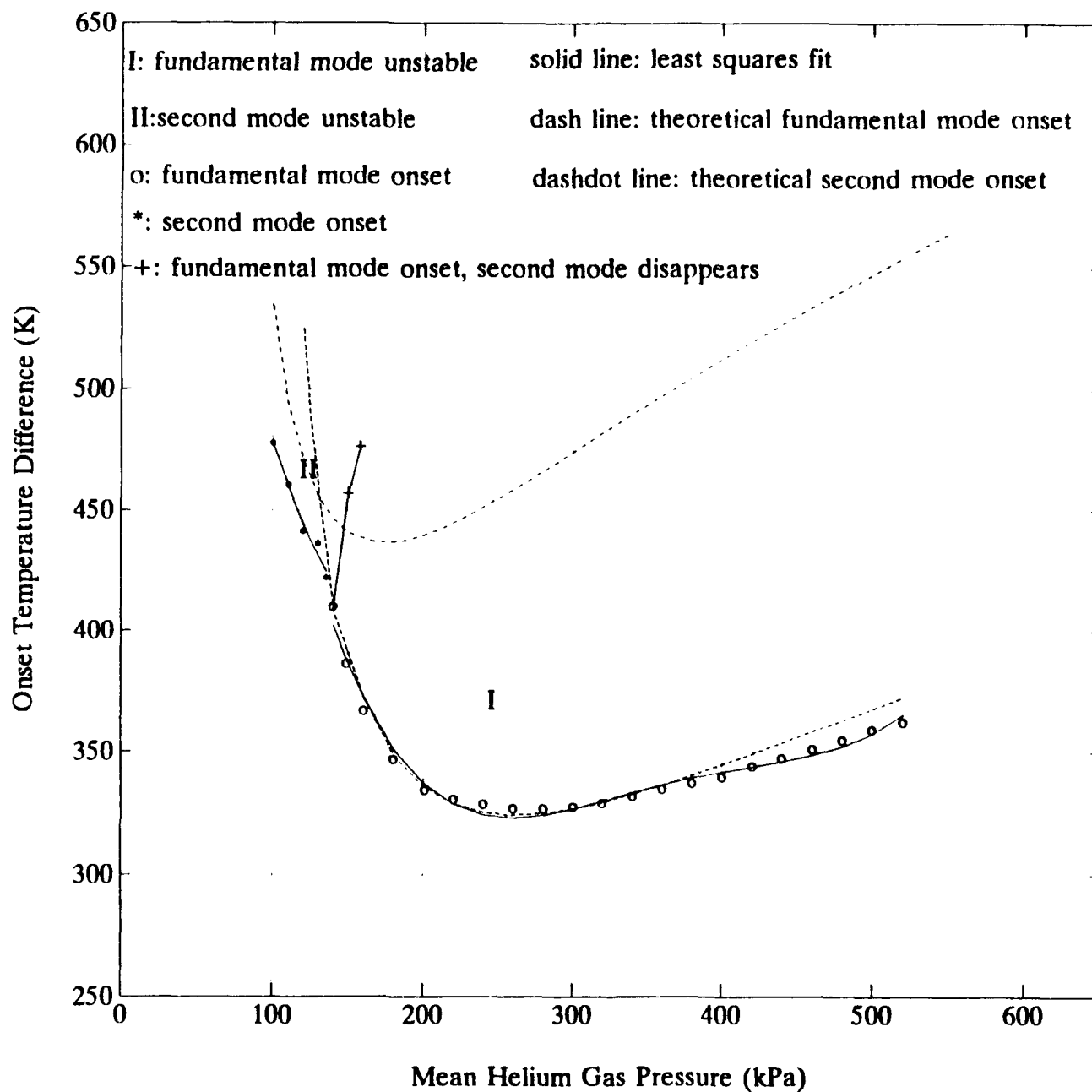


Figure 4 - The stability curves for the fundamental and second modes of a helium filled prime mover.

modes. Apparently the presence of the second mode does, in fact, affect the stability of the fundamental. Note that the slope of the measured low pressure stability limit of the second mode is negative, as predicted. Also note that the second mode is the only one present in this region. In other word, there is no other mode present to interfere with it. One possible interaction is that the presence of the second mode alters the temperature distribution in the stack significantly, so that ΔT is unrepresentative of the actual conditions in the stack. Another possible explanation is that there is nonlinear mode competition between the fundamental and second mode. When the second mode is present, it has the advantage over the fundamental well into the region where the fundamental should be unstable. The behavior of the stability curve of the fundamental at low pressures shows that below approximately 140 kPa, the fundamental mode will *never* be excited, *regardless* of how high ΔT becomes. This result was unexpected.

That one mode can suppress the other is in fact observed and is the second interesting aspect of Fig. 4 mentioned above. The measured stability curve for the second mode does not extend to the right of the intersection with that of the fundamental. In other words, we never observe onset of the second mode once the fundamental is excited. We used two methods to search for second mode onset. In one, we fixed the mean pressure and increase ΔT up to a maximum value of approximately 550 K, well above that which should be required for second mode onset. In the other, we fixed ΔT and increased P_m . In neither case could we see second mode onset.

Equally interesting is what happens to the second mode when the fundamental mode reaches onset. To use a specific example, if ΔT is set to 450 K and P_m is increased from zero, the second mode reaches onset at a pressure of approximately 115 kPa. As P_m is in-

creased further, the amplitude of the second mode increases. When the mean pressure reaches approximately 150 kPa, we see the fundamental mode begin to grow. For a brief period, both modes are simultaneously excited with the amplitude of the fundamental increasing and that of the second mode decreasing. Soon the second mode is completely gone and only the fundamental is left. Further increase of P_m only results in the growth of the fundamental. The second mode never comes back, even though it should be unstable.

To investigate this behavior further, we decided to selectively inhibit the fundamental mode, without affecting the second. This is accomplished by inserting a disc in the prime mover at the location of the velocity antinode of the fundamental mode. The 3.13-mm thick brass disc has a 18.33-mm diameter hole in the center. The idea is that the reduced cross section presents a significant flow impedance to the fundamental mode, thereby raising its ΔT_{onset} . But, because the disc is at near the velocity node of the second mode, the second mode onset conditions will be affected very little. By inhibiting the fundamental, the fundamental's influence on the second mode should be diminished.

The stability curves for the modified prime mover are shown in Fig 5. Two points are immediately evident. First, the stability curve for the fundamental shifts towards higher ΔT and P_m with the disc present. This point is illustrated in Fig. 6 which shows the stability curves for the fundamental mode with and without the disc. In addition to shifting the stability curve, the disc also results in a much lower fundamental amplitude. This apparently allows the second mode to dominate over the fundamental to a larger extent, as indicated by region II occupying more parameter space in Fig. 5 than in Fig. 4. Second, the stability curve for the second mode now extends into the region where the fundamental mode previously dominated. The reduced fundamental amplitude apparently prohibits it

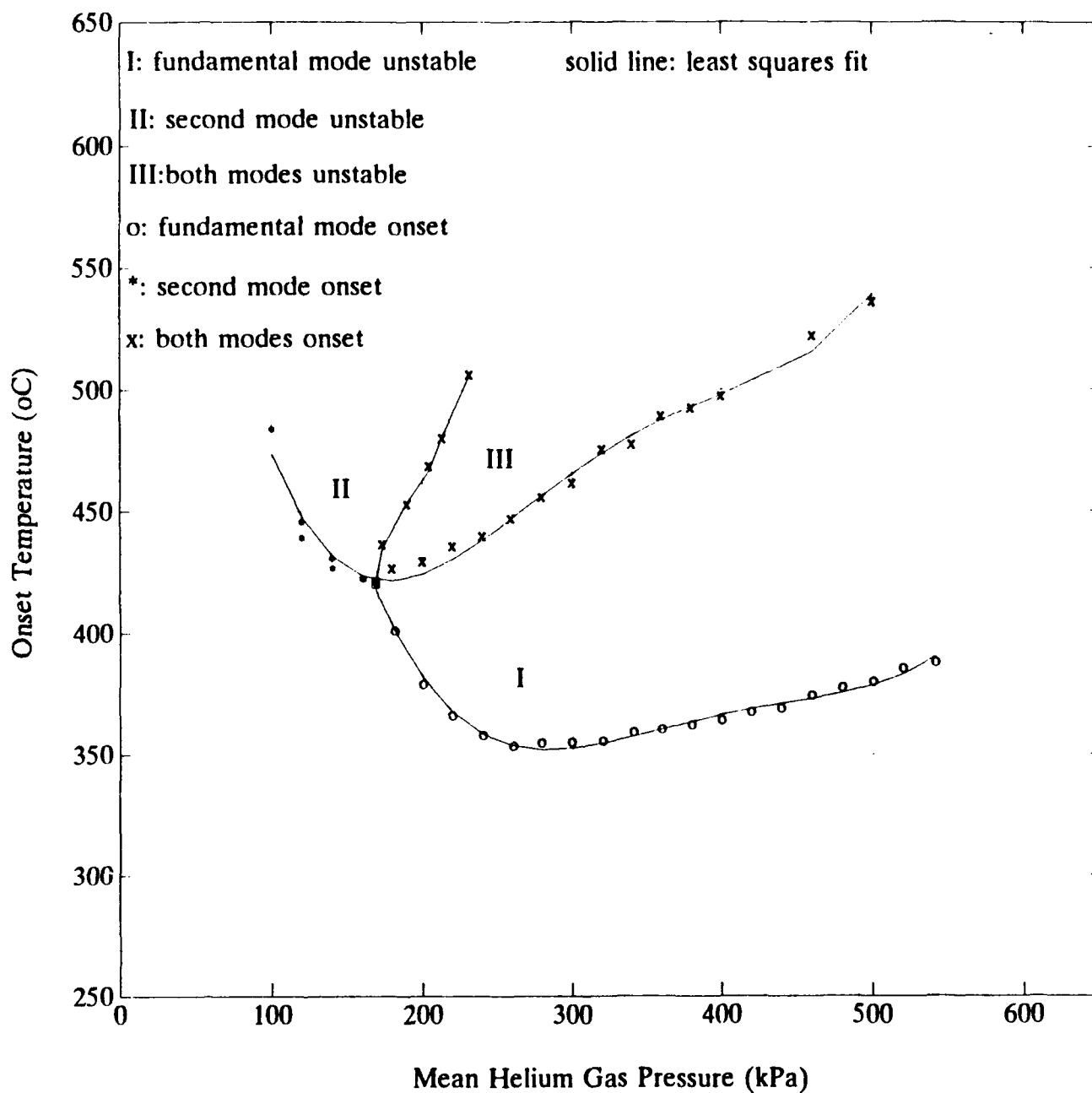


Figure 5 - The stability curves of the modified prime mover.

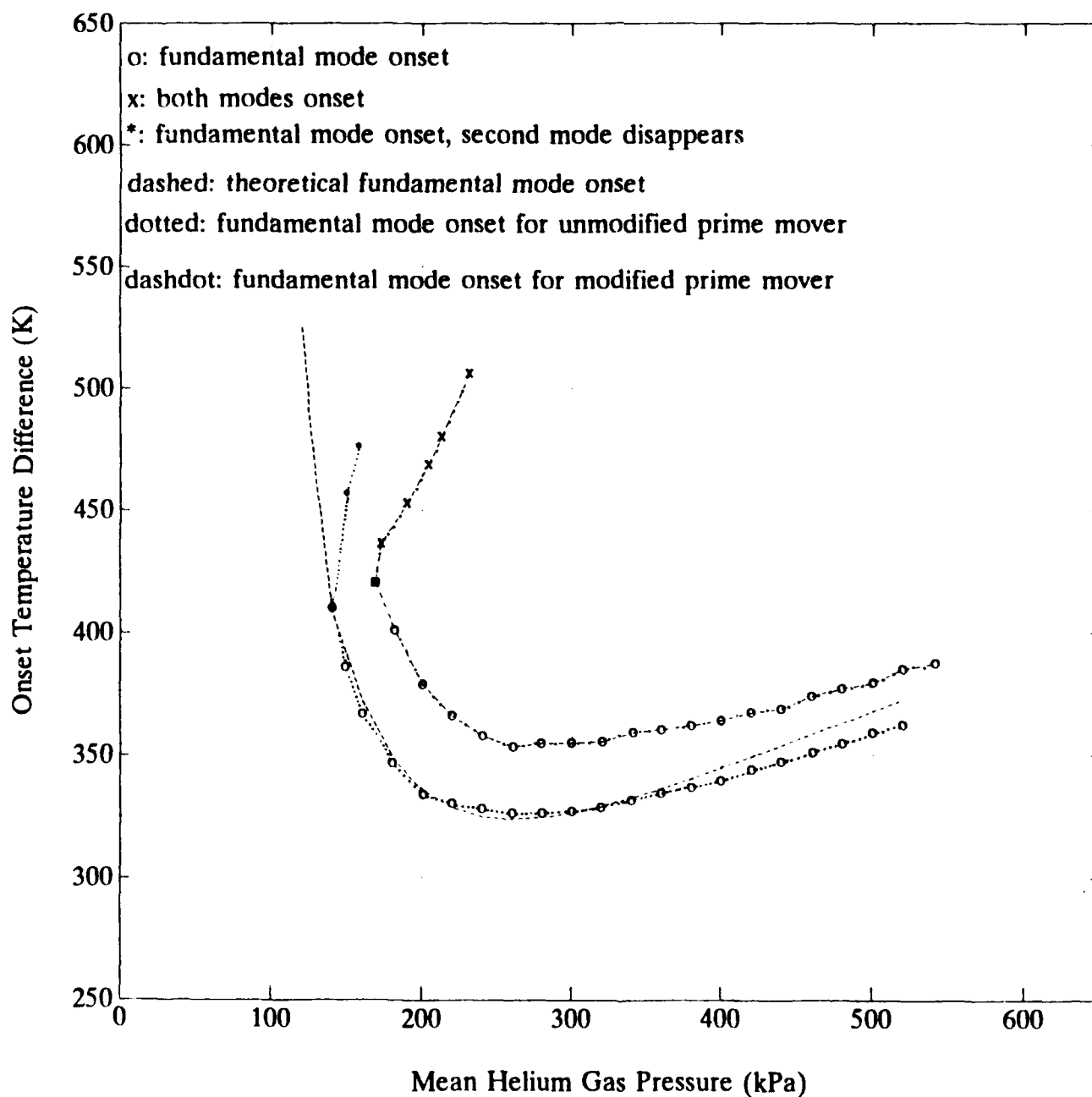


Figure 6 - The stability curves for the fundamental mode of the prime mover with and without the disc.

from dominating the second mode. In the region labeled III, both modes are simultaneously excited.

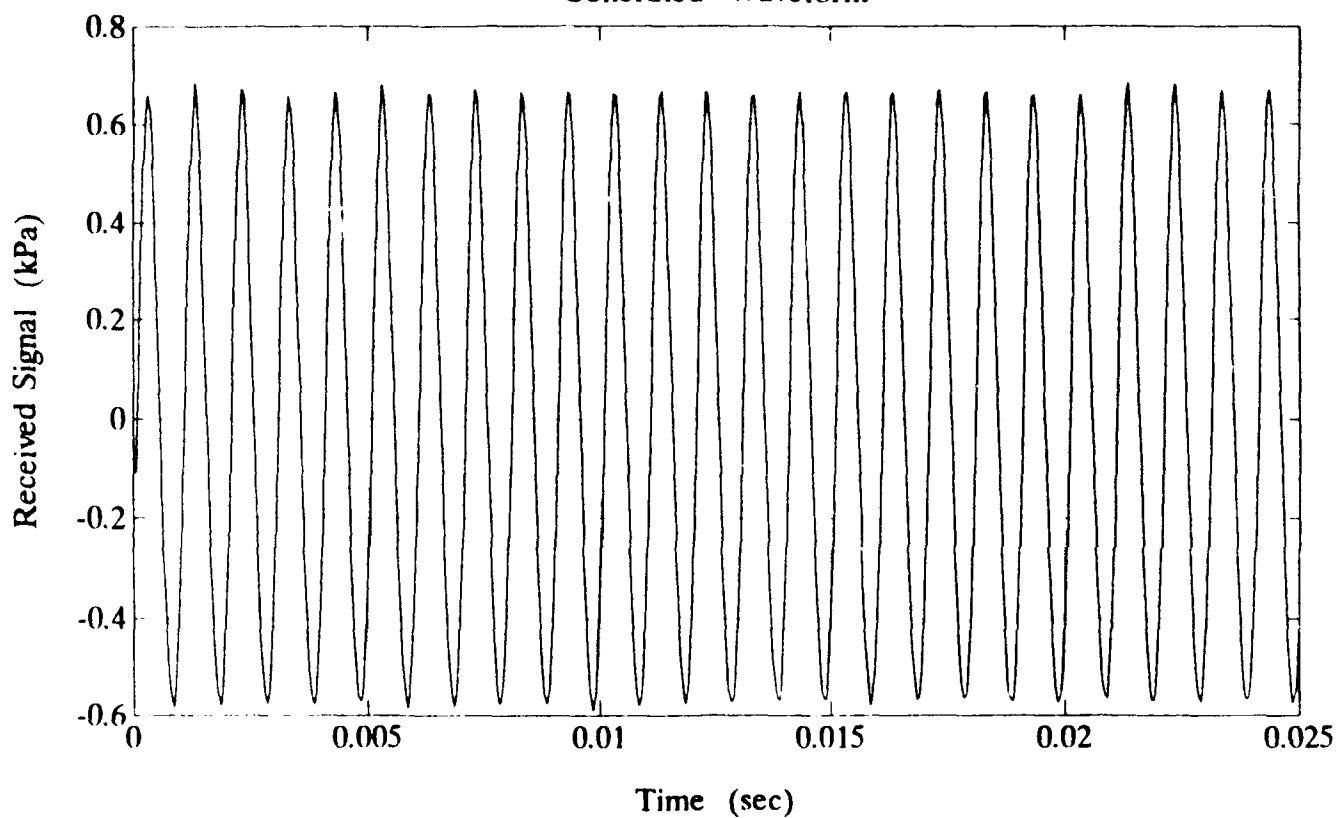
B. ANALYSIS OF WAVEFORMS

We recorded waveforms for the modified prime mover at ΔT equal to 450 K and mean gas pressure of 150, 240 and 440 kPa. These parameters place us in regions I, II and III of Fig. 5. The waveforms, spectra and phase portraits are shown in Figs. 7 - 9.

The point $(P_m, \Delta T) = (150 \text{ kPa}, 450 \text{ K})$ lies in region II, where only the second mode is unstable. The waveform (Fig. 7a) shows a period of approximately 1 ms. The spectrum (Fig. 7b) shows the first harmonic of the signal is at $998.5 \pm 0.6 \text{ Hz}$. The other peaks are harmonics of 998.5 Hz. The phase portraits (Fig. 7c) attest to the periodic nature of the oscillations. The phase traces the same trajectory cycle after cycle, the scatter being due to noise. This point is illustrated by the fact that the solid line which connects the first 100 points of the data and the dots which represent the first 1500 points cover essentially the same area. Similar behavior is observed at the point $(440 \text{ kPa}, 450 \text{ K})$ which lies in region I. The main difference is that in this region only the fundamental mode is excited. The amplitude of this signal (Fig. 8a) is much smaller than that in Fig. 7 and so the signal is noisier. The spectrum (Fig. 8b) indicates that the first harmonic is at $482.2 \pm 0.6 \text{ Hz}$. The phase portrait (Fig. 8c), although showing more scatter due to poorer signal to noise ratio, shows that the waveform is again periodic. The first 100 and the first 1500 points occupy the same area.

The situation is different at the point $(240 \text{ kPa}, 450 \text{ K})$ in region III. In this region both modes are excited simultaneously. This is indicated by a sample of the steady state

Generated Waveform



Sound Pressure Level

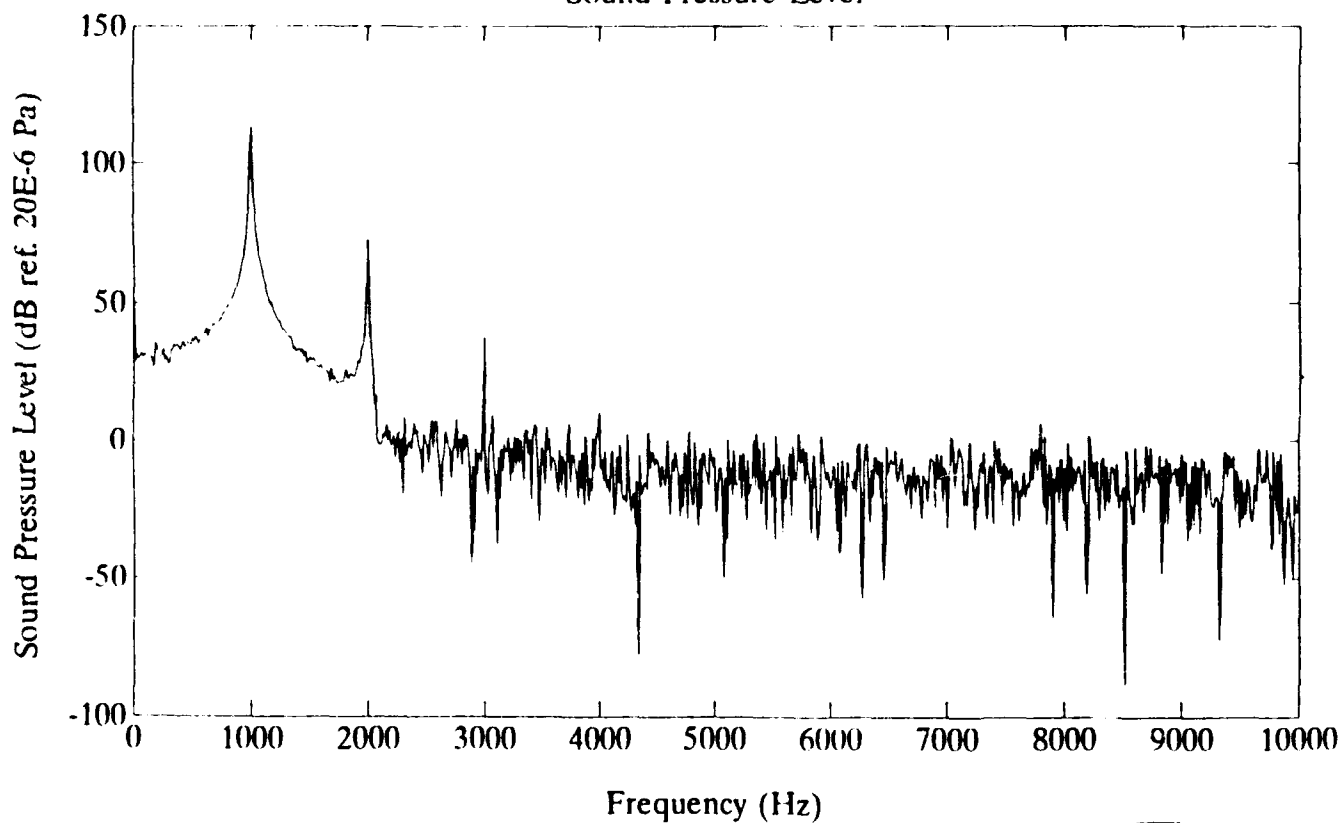


Figure 7a, 7b - The waveform and spectrum for the modified prime mover
at P_m 150 kPa and ΔT 450 K.

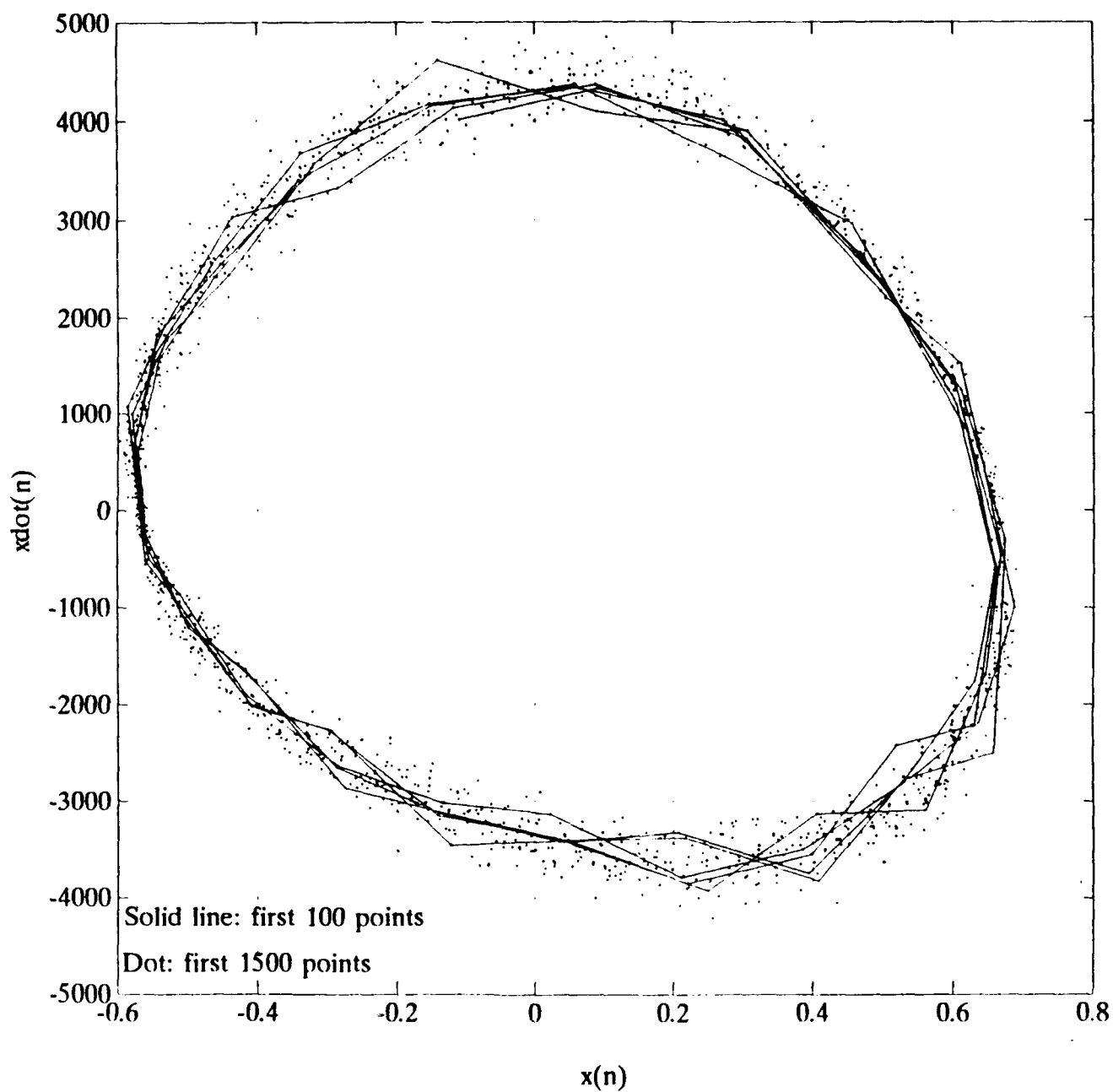
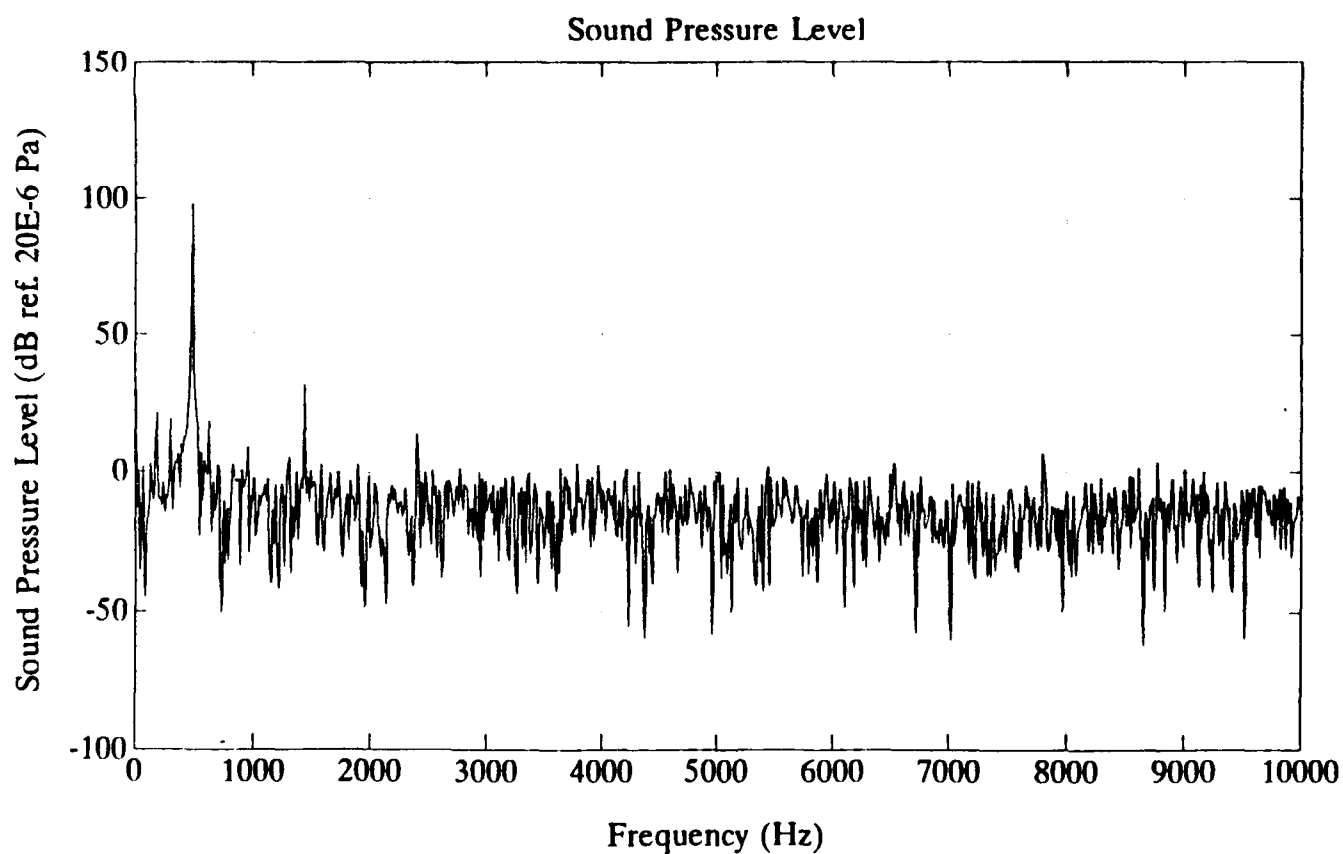
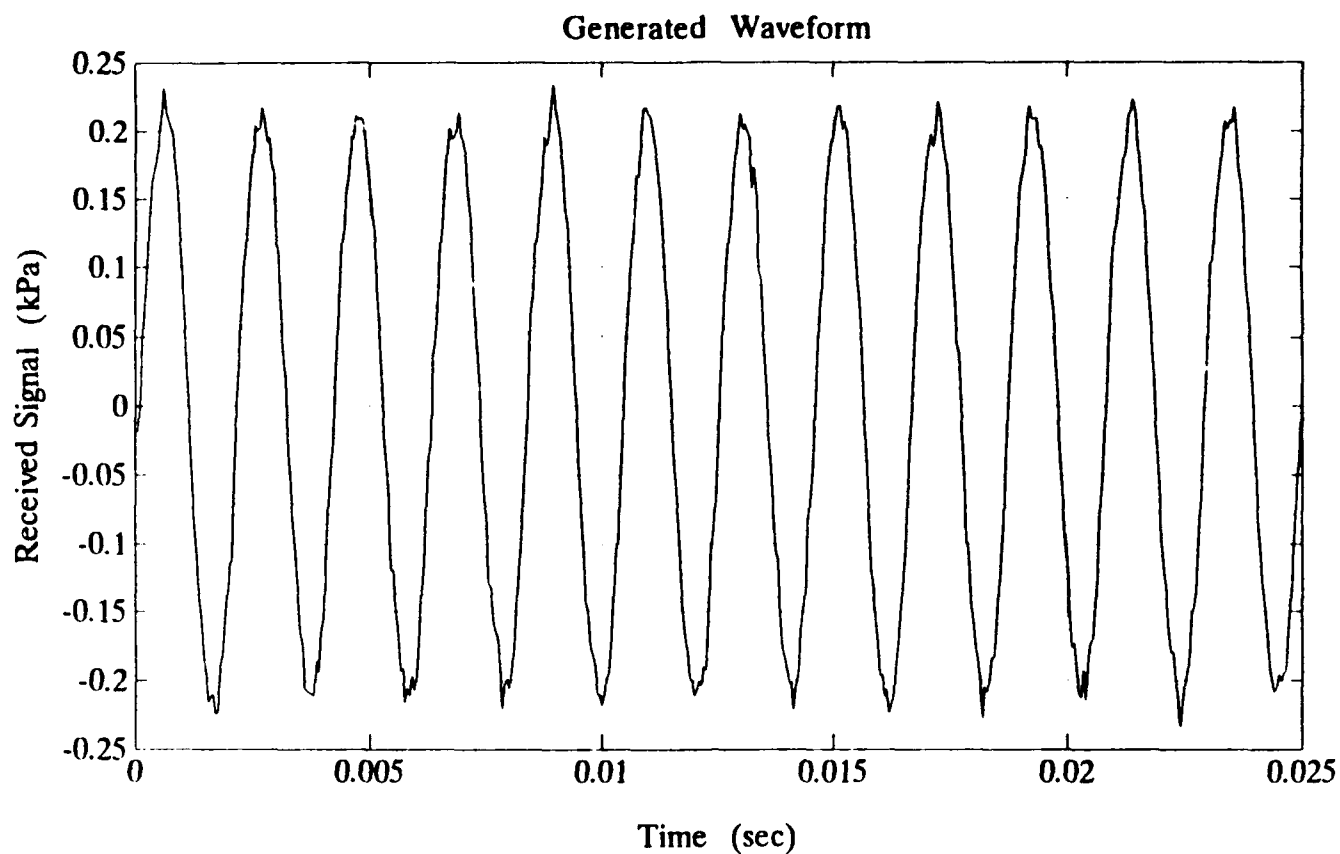


Figure 7c - Phase portrait for the modified prime mover at P_m 150 kPa, ΔT 450 K.



**Figure 8a, 8b - The waveform and spectrum for the modified prime mover
at P_m 440 kPa and ΔT 450 K.**

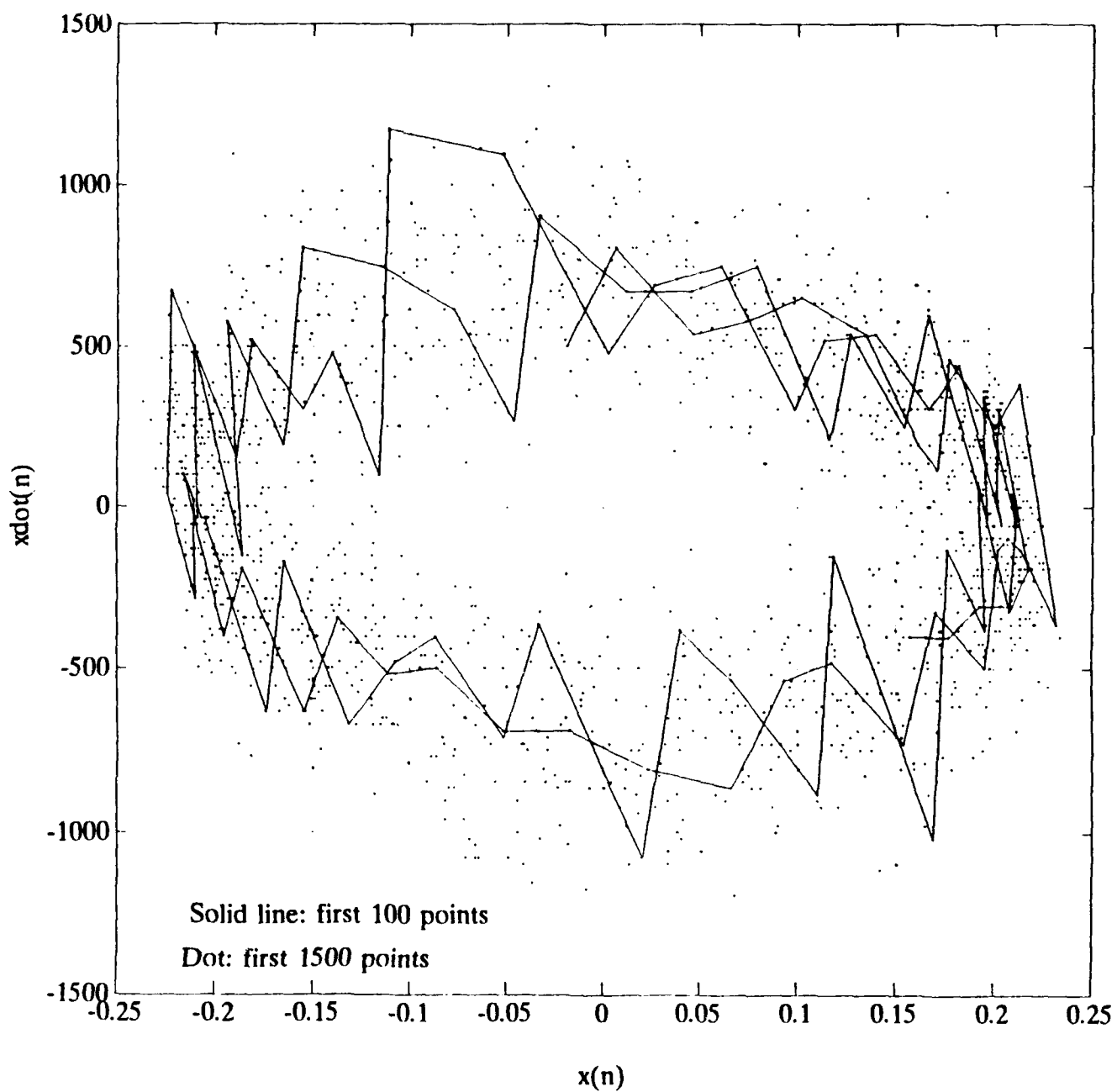


Figure 8c - Phase portrait for the modified prime mover at P_m 440 kPa, ΔT 450 K.

waveform (Fig. 9a) and its spectrum (Fig. 9b). The lowest frequency peak, at 484.0 ± 0.6 Hz, corresponds to the fundamental mode; the second peak, at 996.1 ± 0.6 Hz, corresponds to the second mode. Higher harmonics of both modes are also present. Because the fundamental and second modes are not harmonic, the combination is not periodic. It is quasiperiodic. This point is illustrated by the phase portrait (Fig. 9c). The first 100 points trace out a curve with an inner and outer loop. The two loops indicate the presence of two modes. However, the next 1400 points do not trace over the same area. They fill in the area bounded within some well defined limits. This indicates that the oscillations never exactly repeat. They are not periodic. This behavior is in contrast to that exhibited by the two previous waveforms, which, except for scatter due to noise, trace over the same path cycle after cycle.

The quasiperiodic nature of the oscillations is demonstrated better in Fig. 9d. This graph shows more of the waveform displayed in Fig. 9a. The evidence of the quasiperiodicity is the appearance of an amplitude modulation. This modulation is the result of the addition of the two incommensurate frequencies. The time interval between maxima of the envelop is equal to $1 / (f_2 - 2f_1)$, which is 36 ms for 484 and 996 Hz. The measured period is 36 ms.

Finally, we want to show the difference in the behavior of the modified and unmodified prime mover. Figures 10 - 12 show the waveforms, spectra and phase portraits for approximately the same three points in parameter space for the unmodified prime mover. The stability curve for this case is shown in Fig. 4. One obvious difference is that the amplitude of the oscillation is much larger. The waveforms are highly nonlinear, especially at the point (440 kPa, 450 K). The first mode dominates at all the points. The

phase portraits, although convoluted, indicate that the signals are periodic. This conclusion is also borne out by the observations discussed previously in which the second mode although excited initially is extinguished as the fundamental mode grows. The use of a series of discs with progressively larger holes and progressively larger fundamental amplitudes might be useful in studying this effect in more detail.

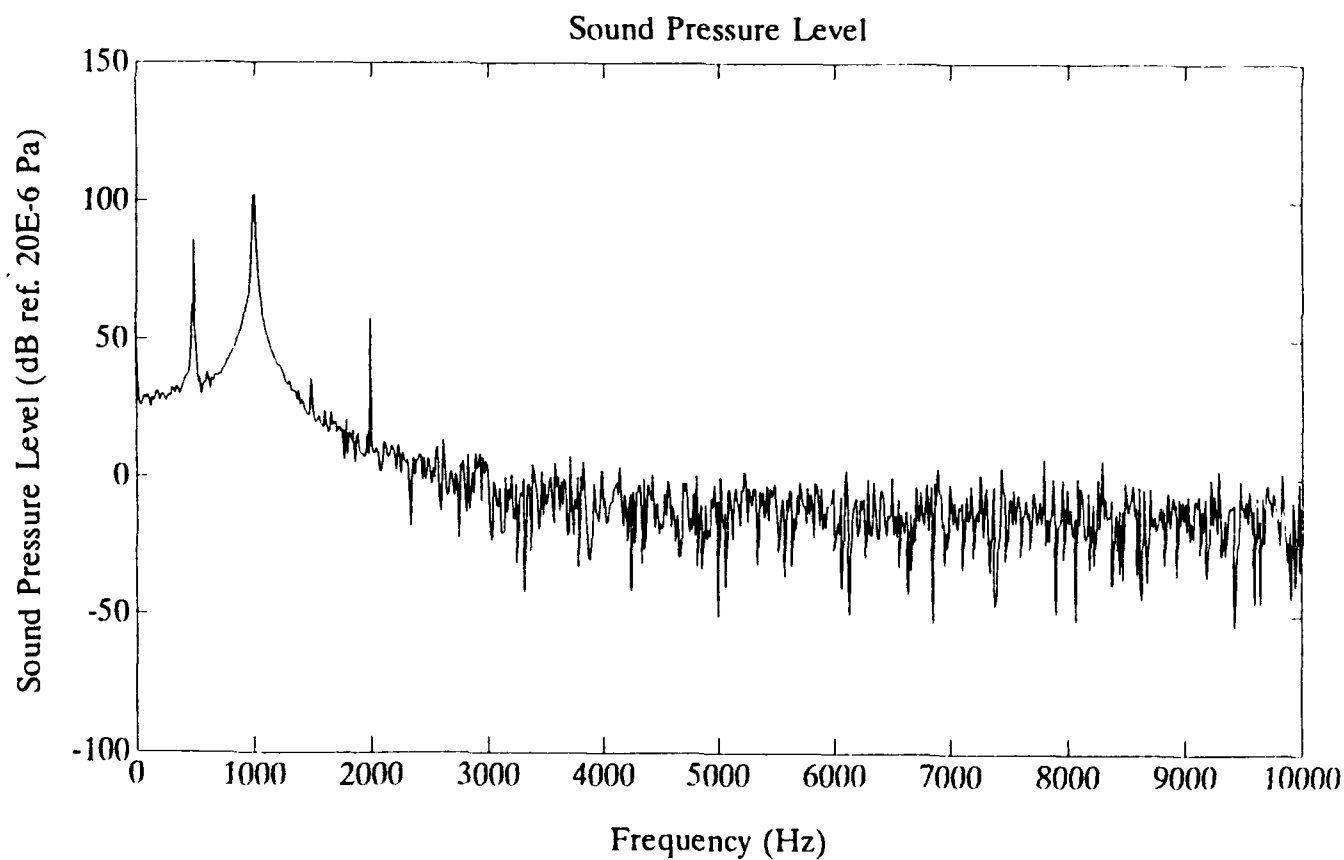
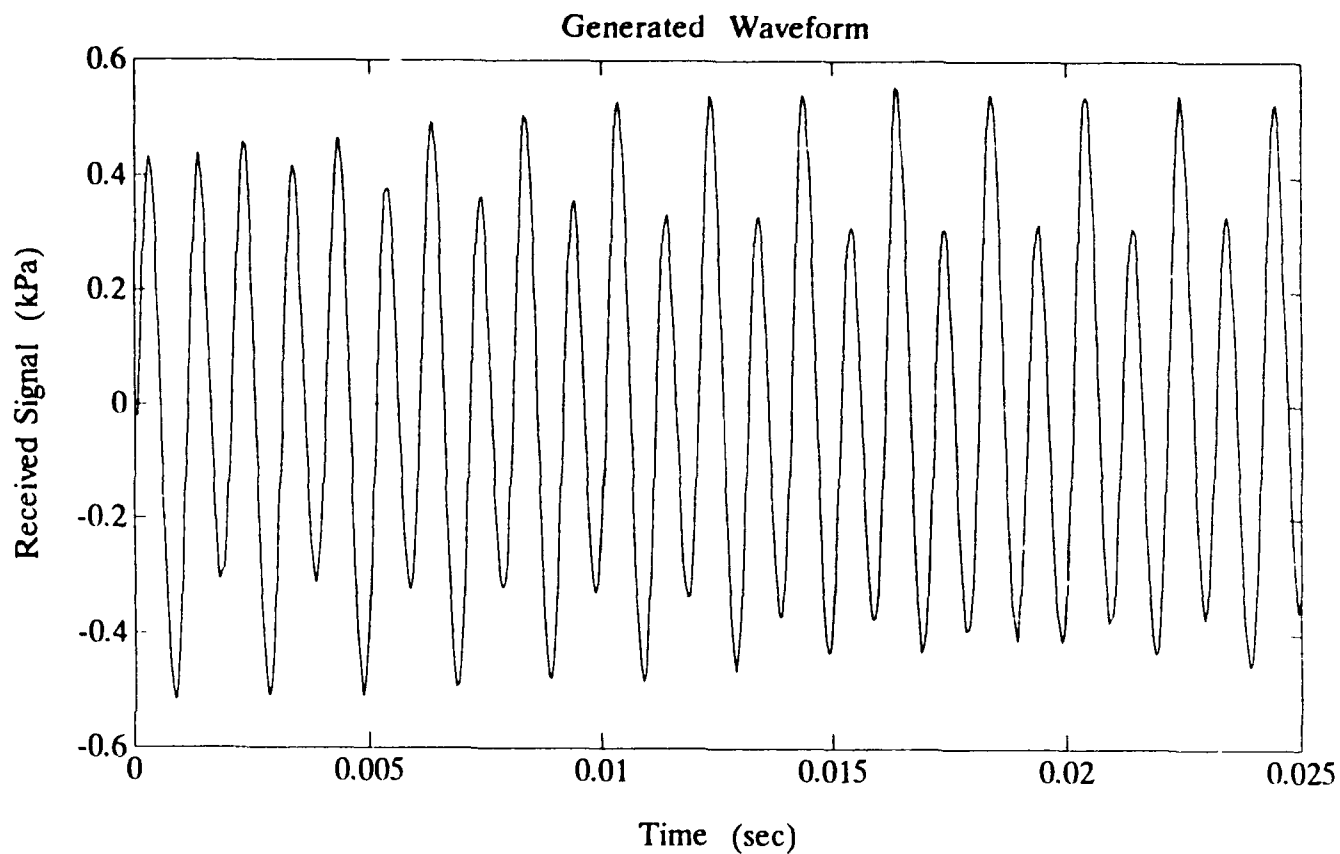


**Figure 9a, 9b - The waveform and spectrum for the modified prime mover
at P_m 240 kPa and ΔT 450 K.**

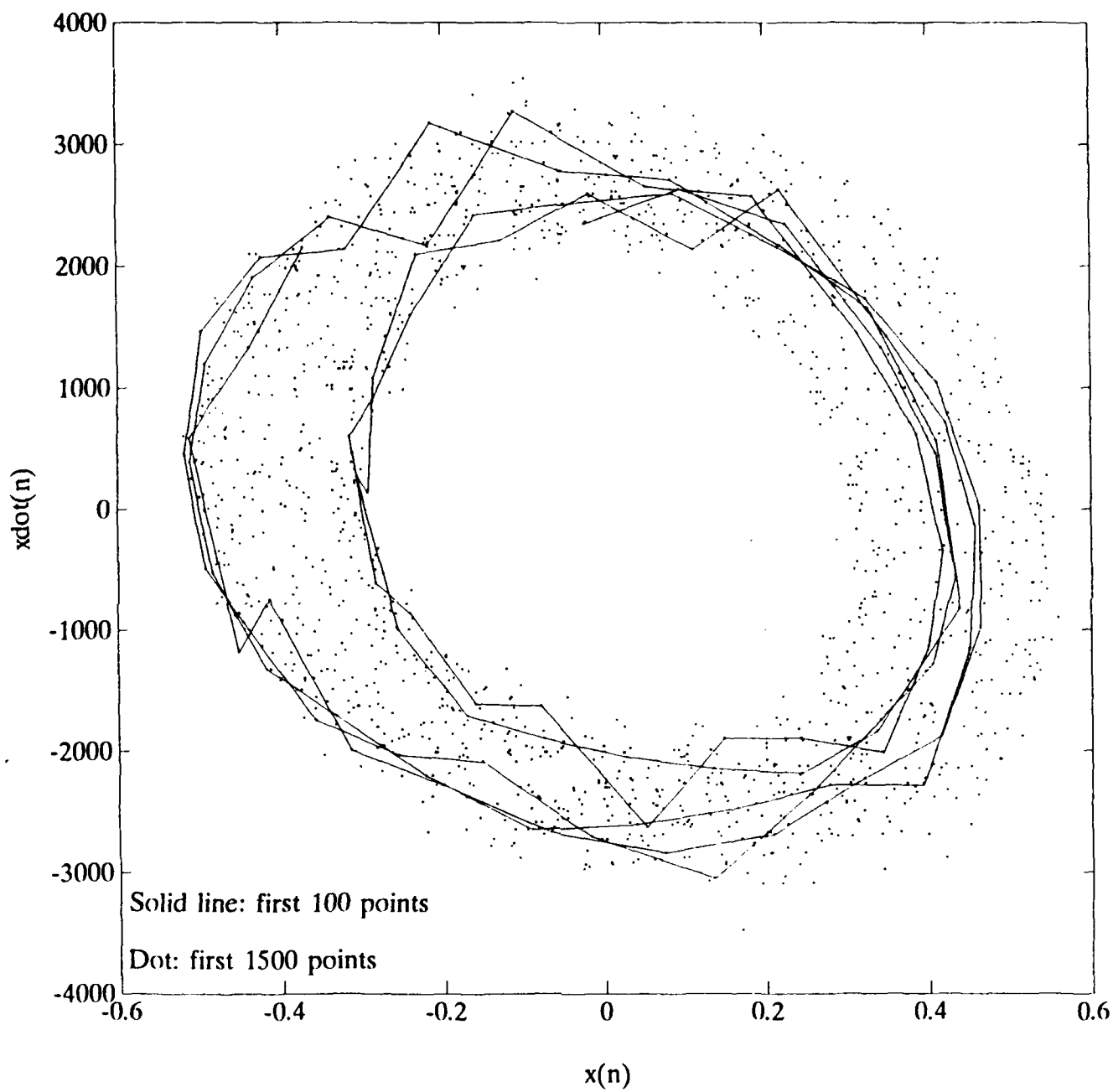


Figure 9c - Phase portrait for the modified prime mover at P_m 240 kPa, ΔT 450 K.

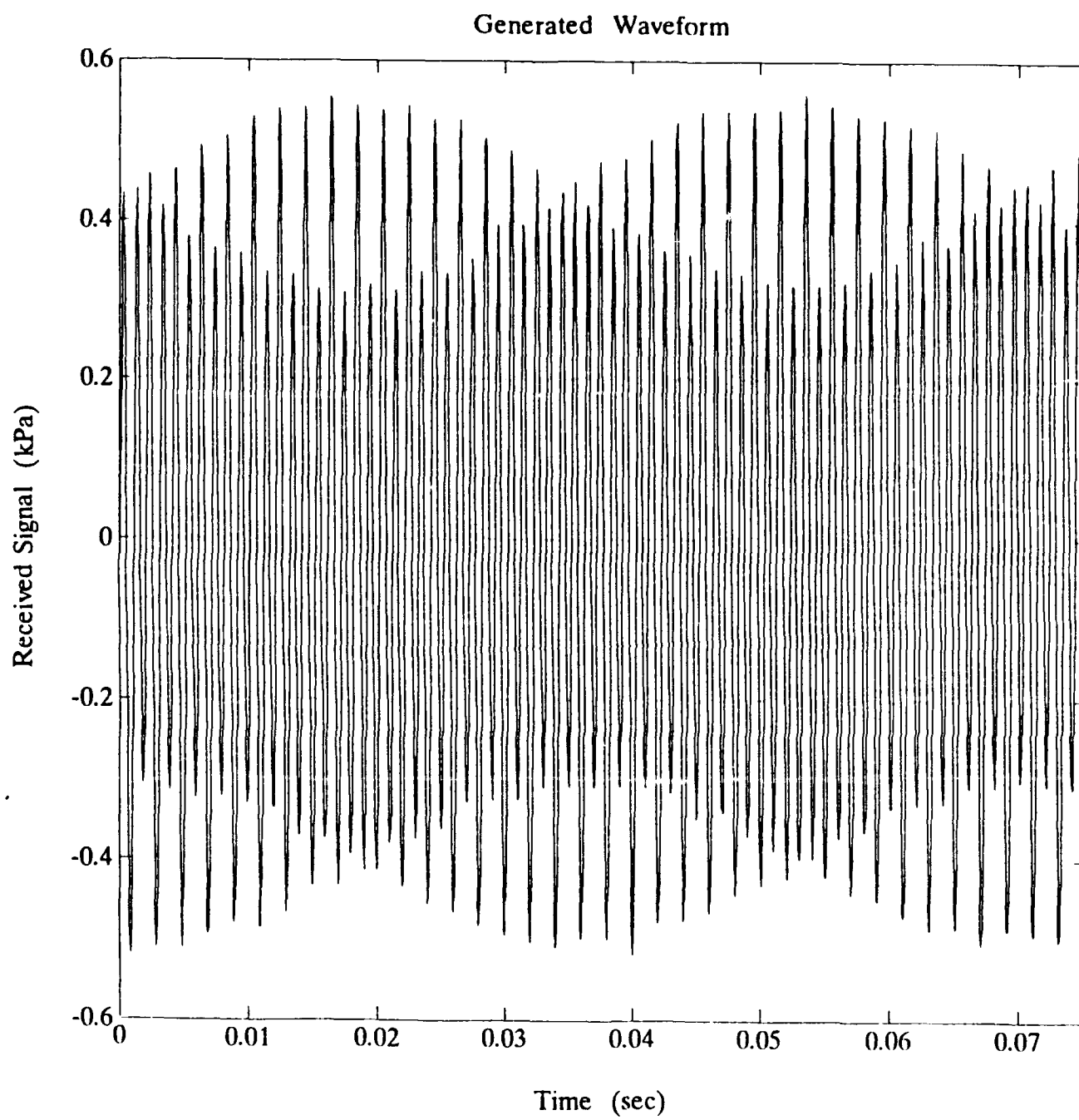


Figure 9d - The waveform for the modified prime mover at P_m 240 kPa and ΔT 450 K.

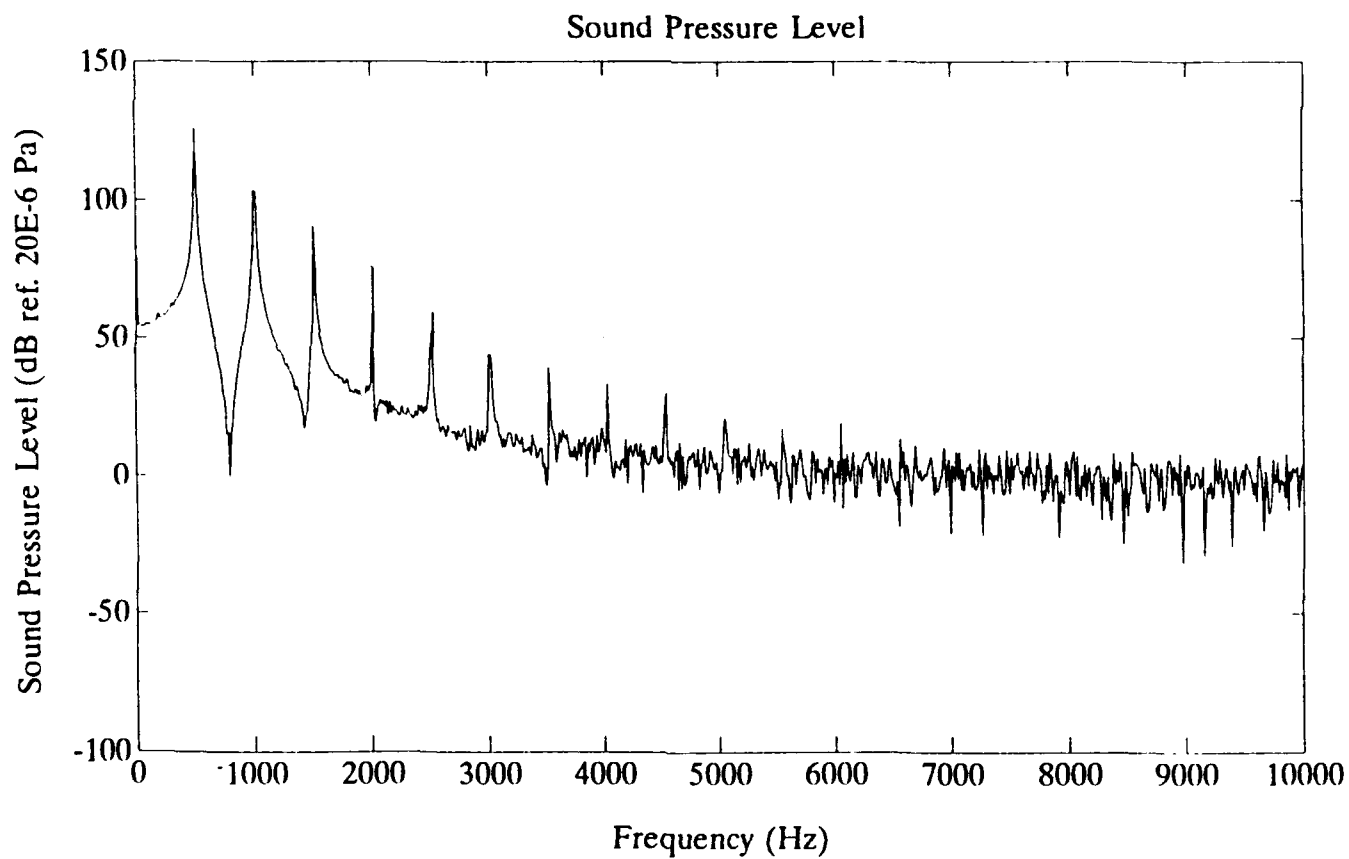
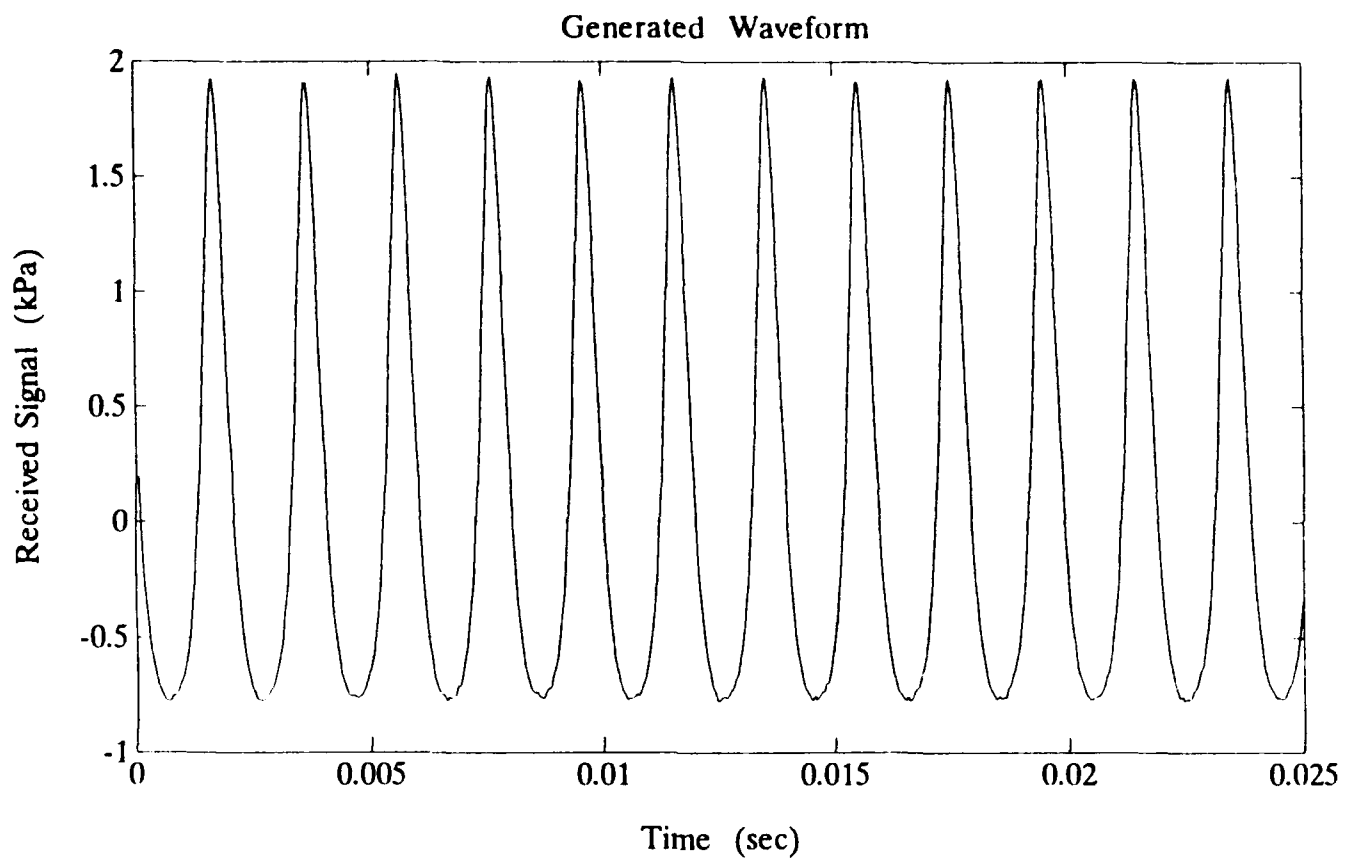


Figure 10a, 10b - The waveform and spectrum for the unmodified prime mover at P_m 150 kPa and ΔT 450 K.

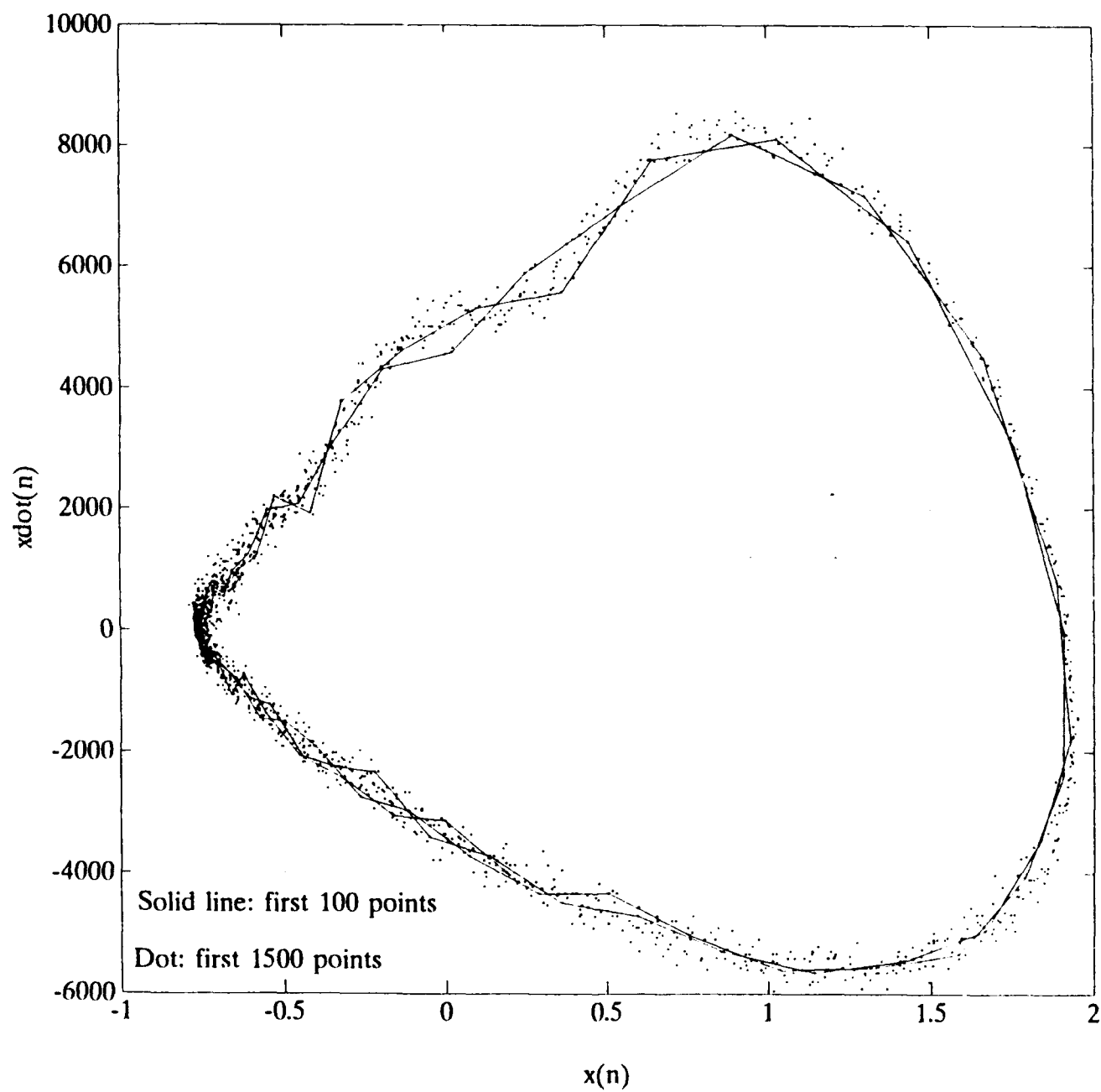


Figure 10c - Phase portrait for the unmodified prime mover at P_m 150 kPa, ΔT 450 K.

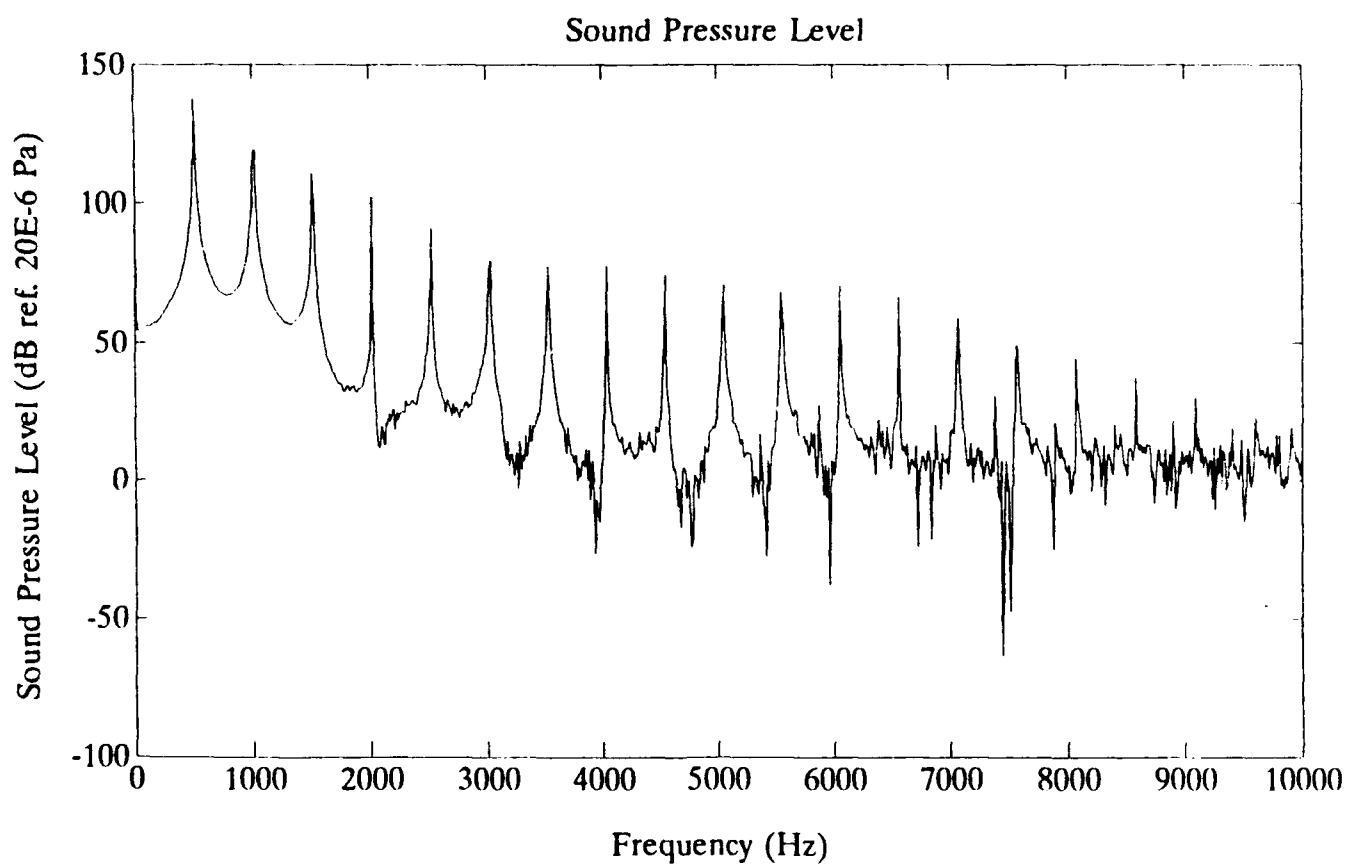
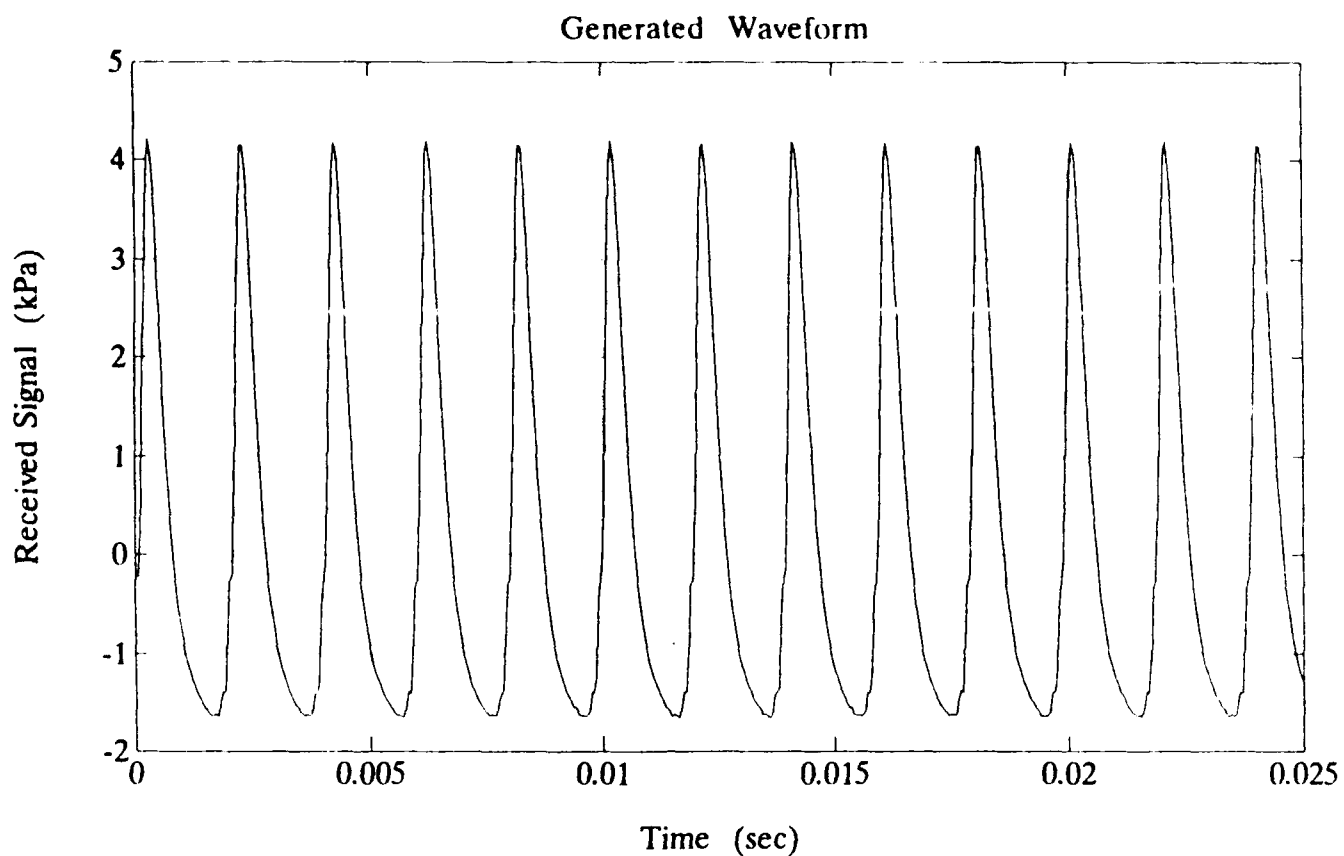


Figure 11a,11b - The waveform and spectrum for the unmodified prime mover at P_m 240 kPa and ΔT 450 K.

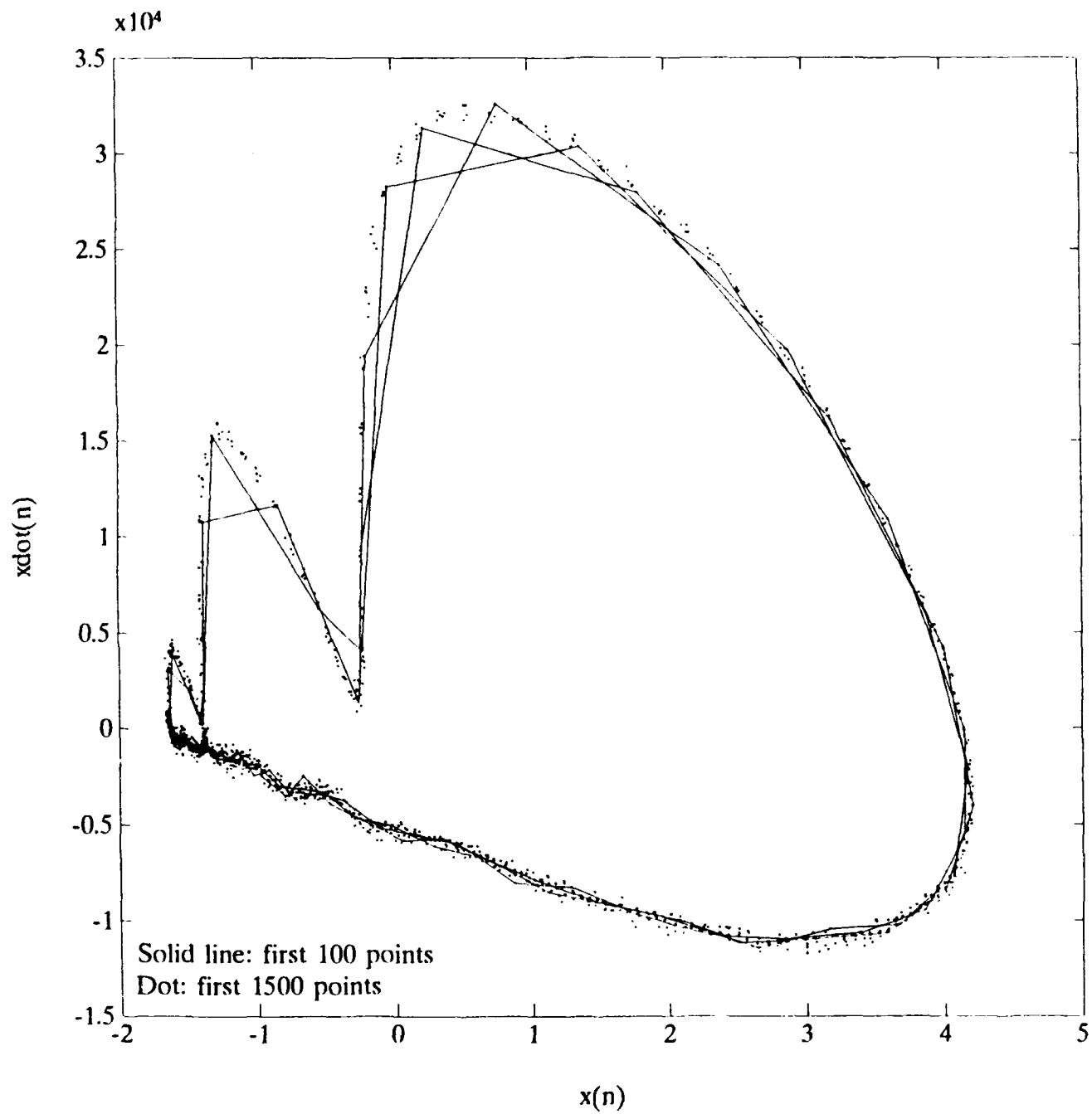


Figure 11c - Phase portrait for the unmodified prime mover at P_m 240 kPa, ΔT 450 K.

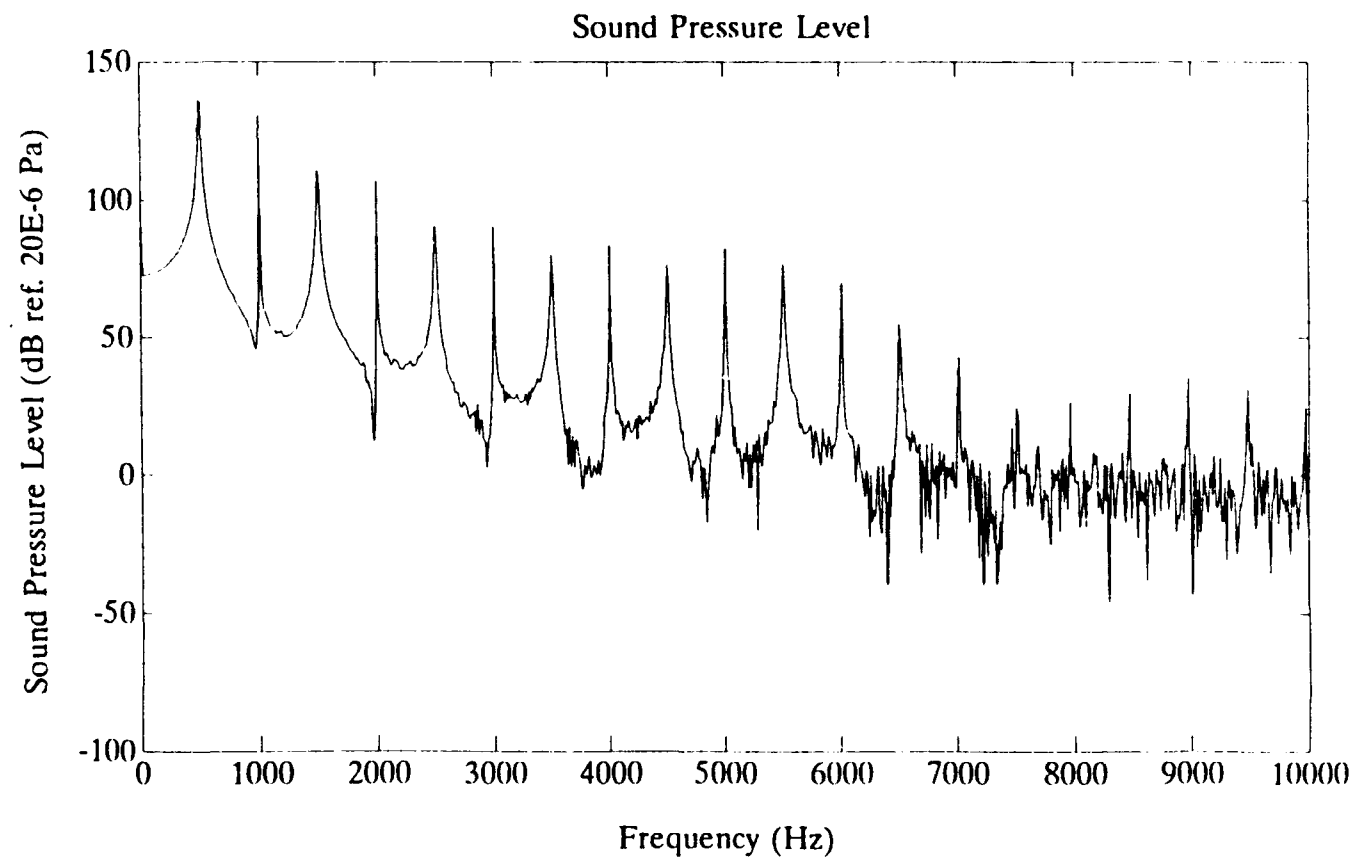
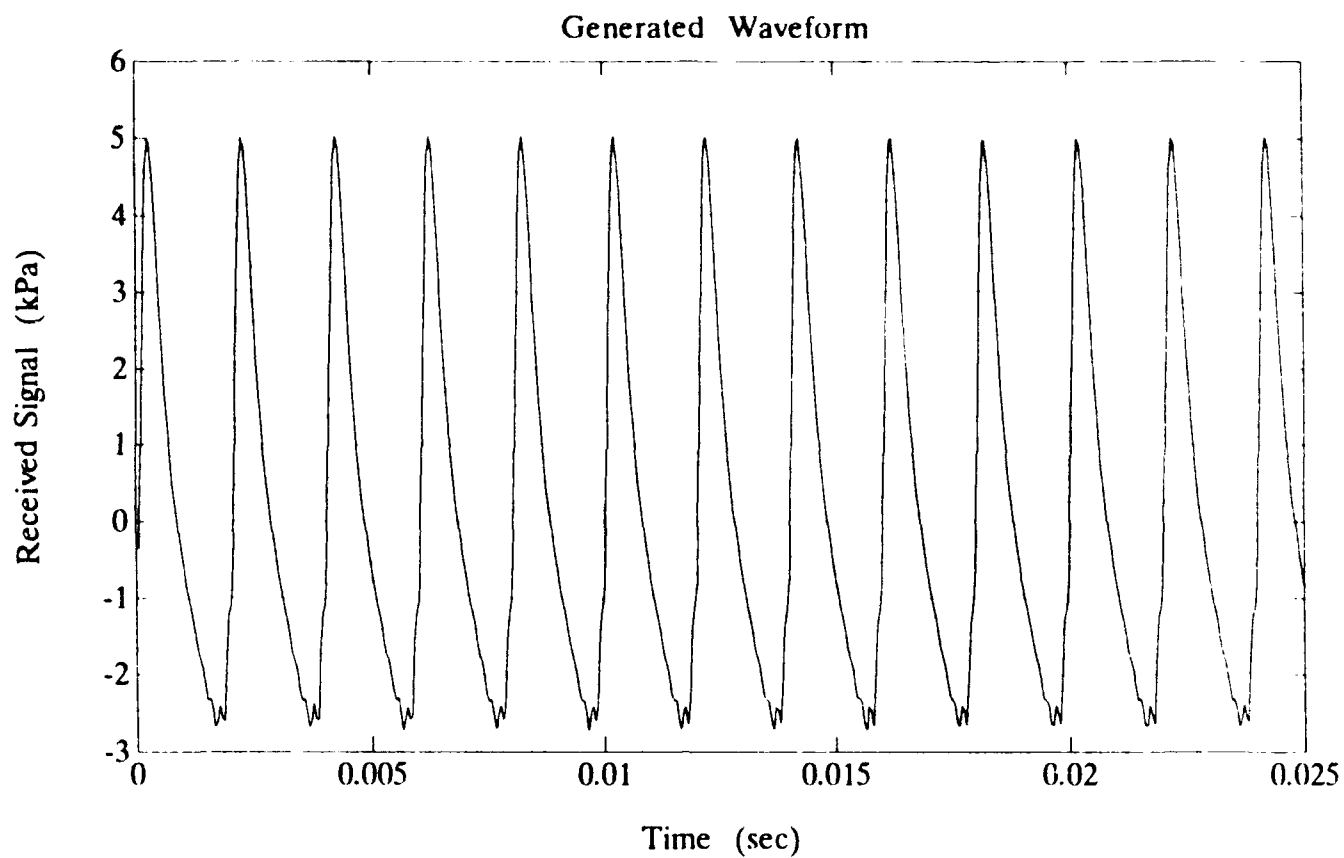


Figure 12a, 12b - The waveform and spectrum for the unmodified prime mover at P_m 440 kPa and ΔT 450 K.

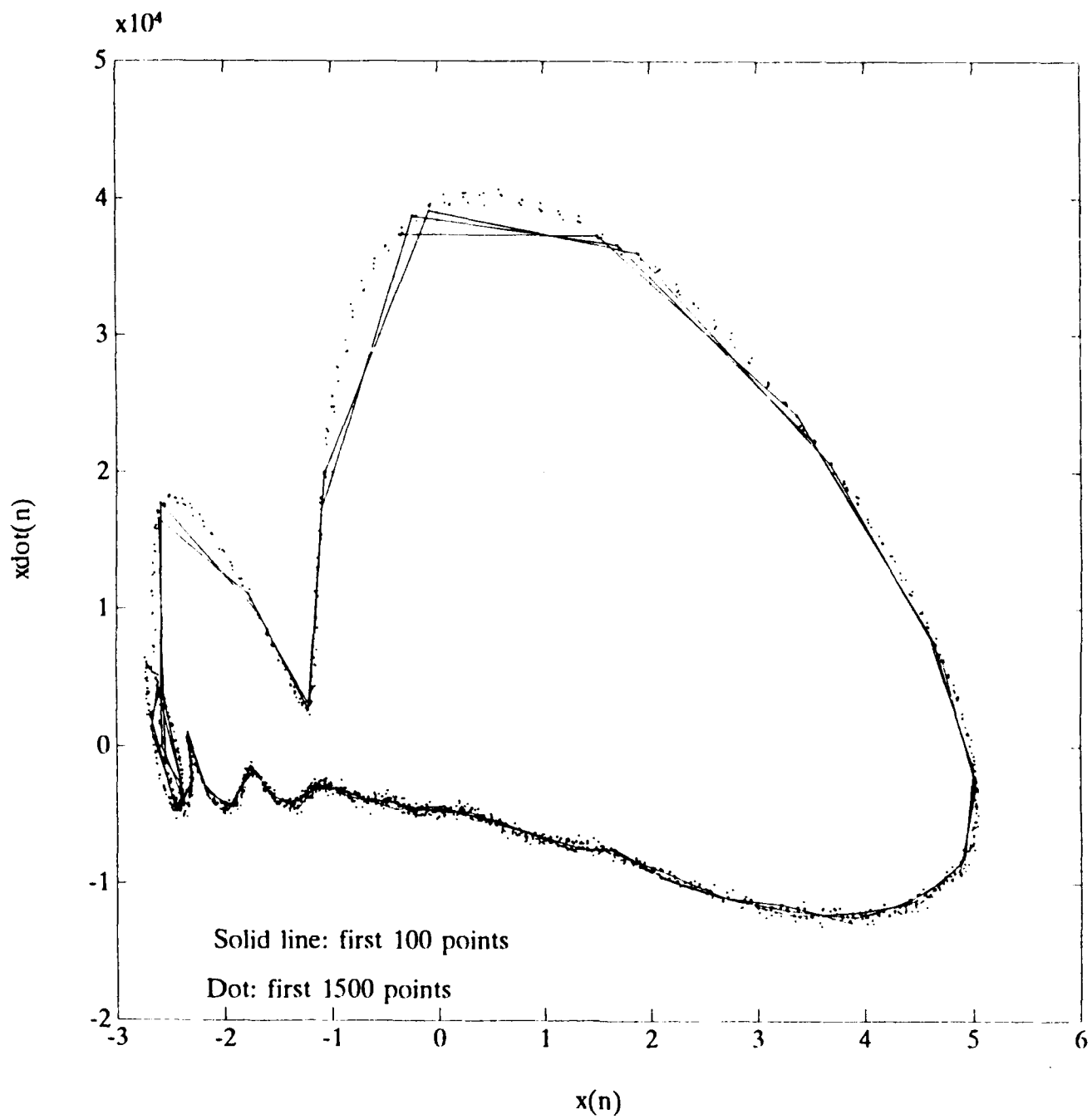


Figure 12c - Phase portrait for the unmodified prime mover at P_m 440 kPa, ΔT 450 K.

V. SUMMARY AND RECOMMENDATIONS

A. SUMMARY

The purpose of this thesis is to investigate the stability curves and steady state waveforms of a helium filled prime mover. We measured the stability curves for both the fundamental and second modes. The agreement between the predicted and measured stability limits is within a few percent for the fundamental mode at most mean pressures. The predicted trend for the second mode is also consistent with the measurements, although the predicted value of ΔT_{onset} is consistently higher than that measured. A more interesting aspect of the measurements is that the stability of one mode is affected by the presence of the other. In fact, the stability curve of the fundamental at low pressures shows that below approximately 140 kPa, the fundamental mode will never be excited, regardless of how high ΔT becomes. This unexpected conclusion is in contradiction to predictions and is apparently due to the fact that the second mode is above onset in this region of parameter space.

It is also observed that one mode can suppress the other. The measured stability curve for the second mode does not extend to the right of the intersection with that of the fundamental. In other words, we never observe onset of the second mode once the fundamental is excited. Equally interesting is what happens to the second mode when the fundamental mode reaches onset. We observe a brief period where both modes are simultaneously excited with the amplitude of the fundamental increasing and that of the second mode decreasing. Soon the second mode is completely gone and only the

fundamental is left. Further increase of P_m only results in the growth of the fundamental. The second mode never comes back, even though it should be unstable.

To investigate this behavior further, we decided to selectively inhibit the fundamental mode, without affecting the second. This is accomplished by inserting a disc in the prime mover at the location of the velocity antinode of the fundamental mode. Measurements of the modified prime mover show that the stability curve for the second mode now extends into the region where the fundamental mode previously dominated. There is also a region where both modes are simultaneously excited. Analysis of the waveforms show that the resulting oscillations are quasiperiodic.

B. RECOMMENDATIONS

The results of this thesis point to several areas for further work. First, there is need for a model that accurately predicts the stability curves by accounting for the interaction between modes. Also, measurements of the stability curves in parameter regions where both modes exist may prove to be a useful testbed for various thermoacoustics models. Finally, a more extensive investigation of $(P_m, \Delta T)$ parameter space may reveal regions of more complex behavior such as chaos. Such a study may lead to novel applications regarding control of oscillations in prime movers.

LIST OF REFERENCES

1. Anthony A. Atchley, "Standing Wave Analysis of a Thermoacoustic Prime Mover Below Onset of Self-Oscillation," *J. Acoust. Soc. Am.* **92(5)**, 2907-2914 (1992).
2. Lin, Hsiao-Tseng, "Investigation of a Heat Driven Thermoacoustic Prime Mover," Master's Thesis, Naval Postgraduate School, Monterey, California, December 1989.
3. Anthony A. Atchley et. al., "Study of a Thermoacoustic Prime Mover Below Onset of Self-Oscillation," *J. Acoust. Soc. Am.* **91(2)**, 734-743 (1992).
4. T. Yazaki, A. Tominaga, and Y. Narahara, "Experiments on Thermally Driven Acoustic Oscillations of Gaseous Helium," *J. Low Temp. Phys.* **41**, 45-60 (1980).
5. T. Yazaki, A. Tominaga, and Y. Narahara, "Thermally Driven Acoustic Oscillations: Second-Harmonic," *Phys. Rev. Lett.* **79A**, 407-409 (1980).
6. T. Yazaki, S. Takashima, and F. Mizutani, "Complex Quasiperiodic and Chaotic States Observed in Thermally Induced Oscillations of Gas Columns," *Phys. Rev. Lett.* **58**, 1108-1111 (1986).
7. N. H. Packard, J. P. Crutchfield, J. D. Farmer, and R. S. Shaw, "Geometry from a Time Series," *Phys. Rev. Lett.* **45**, 712-715 (1980).

INITIAL DISTRIBUTION LIST

	No. Copies
1. Defense Technical Information Center Cameron Station Alexandria, VA 22304-6145	2
2. Dudley Knox Library, Code 0152 Naval Postgraduate School Monterey, CA 93943-5100	2
3. Prof. Anthony A. Atchley, Code PH/Ay Department of Physics Naval Postgraduate School Monterey, CA 93943	4
4. Prof. Robert M. Keolian, Code PH/Kn Department of Physics Naval Postgraduate School Monterey, CA 93943	1
5. Dr. Logan E. Hargrove, Code 3120 Physics Division Office of Naval Research 800 North Quincy Street Arlington, VA. 22217-5660	1

- | | |
|---|-------|
| 6. Dr. Felipe Gaitan | 1 |
| Department of Physics | |
| Naval Postgraduate School | |
| Monterey, CA 93943 | |
|
7. LT Kuo, Fan-Ming |
1 |
| No. 57-28 Ming-Fu Road, Pu-Li, Nen-Tou County, Taiwan | |
| R.O.C. | |
|
8. Library of Chinese Naval Academy |
1 |
| P.O. Box 8494 Tso-Ying, Kaohsiung, Taiwan | |
| R.O.C. | |
|
9. Library of Chung-Cheng Institute of Technology |
1 |
| Tashih, Tao-Yuan, Taiwan | |
| R.O.C. | |